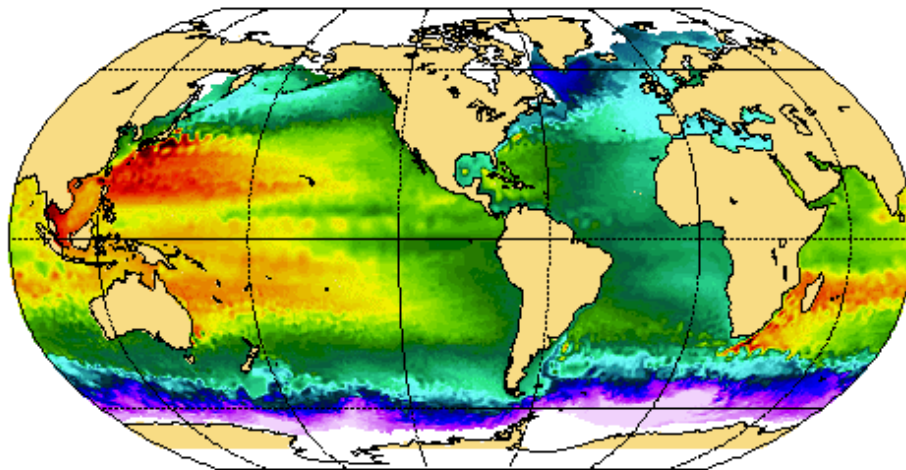




DRAKKAR Project

Variability of the subpolar Atlantic and the Southern Ocean : Local processes and Interactions with the Global Ocean.



Report of Activity 2005-2006
LEGI, LPO, LOCEAN
With contributions from MERCATOR-Océan, LSCE and LEGOS

Décembre 2006

Rapport LEGI-DRA-4-12-2006
Equipe MEOM, Laboratoire des Ecoulements Géophysiques et Industriels, BP53, 38041
Grenoble Cedex 9

Table of Content

1. Scientific Objectives and Modelling Approach -----	3
1.1. Scientific objectives	
1.2. Modelling approach	
2. Project organisation -----	3
2.1. Drakkar concept	
2.2. Drakkar project-team	
2.3. Associate Scientists	
2.4. Cooperation with scientists outside the project	
3. DRAKKAR model configurations -----	5
4. DRAKKAR Project: Report of Activity 2006 -----	8
4.1. Improvement of DRAKKAR model configurations -----	8
4.1.1. <i>Parameterisations</i>	
4.1.2. <i>Momentum advection</i>	
4.1.3. <i>Atmospheric forcing: Definition of DFS3</i>	
4.2. Long simulations of the global variability -----	16
4.2.1. <i>Run ORCA05-G50 : a 56 year long simulation from 1949 to 2004</i>	
4.2.2. <i>ORCA025-G70: a 47 year long simulation from 1958 to 2004</i>	
4.2.3. <i>Analysis of model simulations with regard to observations</i>	
4.3 Dynamics of the Southern Ocean -----	26
4.3.1. <i>Correction for Katabatic Winds</i>	
4.3.2. <i>Antarctic circumpolar ocean dynamics</i>	
4.4. Regional model configurations -----	25
4.4.1. <i>AMEN configuration (Atlantic Mode water in Embedded model using Nemo/agrif)</i>	
4.4.2. <i>Simulation of the isotopic composition of Neodymium.</i>	
4.4.3. <i>Water mass transformations in the Indonesian throughflow</i>	
4.4.4. <i>Modelling biweekly oscillations in the Gulf of Guinea</i>	
4.5. Studies carried out with Associate Scientists -----	30
4.5.1. <i>Transient Tracers</i>	
4.5.2. <i>Ensemble study of the vertical transmission of atmospheric induced temperature anomalies</i>	
4.5.3. <i>Agrifmex</i>	
5. DRAKKAR Publications in 2006 -----	33
6. Personnel -----	35
ANNEXES -----	37

1. Scientific Objectives and Modelling Approach

1.1. Scientific objectives

The primary concern of DRAKKAR is related to the circulation and the day-to-decade variability in the North Atlantic Ocean, as driven by the atmospheric forcing, by interactions between processes of different scales, by exchanges between basins and regional circulation features of the North Atlantic (including the Nordic Seas), and by the influence of the world ocean circulation (including the Arctic). New scientific objectives have emerged in the past two years relative to the variability of the Southern Ocean. DRAKKAR is also concerned by the role of the changing ocean circulation in ecosystem dynamics, and in climate through the transport of heat and freshwater and the uptake of atmospheric CO₂.

1.2. Modelling approach

The scientific approach of the teams participating in DRAKKAR mainly relies upon numerical simulations. Therefore, the project has built a hierarchy of embedded model configurations, based on the NEMO code (<http://www.lodyc.jussieu.fr/NEMO/>), able to provide continued and systematic development and assessment of the ocean model components used in ecosystem, carbon cycle, and climate studies as well as in regional and operational oceanographic applications. The various DRAKKAR configurations will be run for multiple decades to provide a relevant, four-dimensional description of the atmospherically driven world ocean circulation and variability over the last 50 years. This description will allow (in the limits of model accuracy) to study the regional impacts of the global oceanic variability during this period, and to identify remote interactions between the North Atlantic and the World Ocean. It is also expected to contribute to the interpretation of the changes noticed in past and future ocean observations.

2. Project organisation

2.1. Drakkar concept

During the last decade, the DRAKKAR participating scientists fostered co-operative scientific activities within the Mast3 European project DYNAMO (Dynamics of North Atlantic Models), and between their national projects, CLIPPER in France and FLAME (Family of Linked Atlantic models) in Germany. The expertise gained through projects such as these also helped to build their capability to make significant contributions to a variety of modelling needs. However, the challenge of developing realistic ocean models required for the diverse range of applications can only be met by an effective integration and co-ordination of the activities and complementary expertise of every member of the group. This fact yielded the DRAKKAR concept. The project is organised with an international project-team comprising research groups in France, Germany, and Russia, and associated scientists who cooperate with the project.

2.2. Drakkar project-team

Scientists participating to the Drakkar project-team are from 8 different laboratories; LEGI in Grenoble, LPO in Brest, LOCEAN in Paris, MERCATOR-Ocean in Toulouse, LSCE in Orsay, IFM-Geomar in Kiel, and Shirshov Institute of Oceanography (SIO) in Moscow. The project-team conducts the project activities. It has the charge to define details of the model configurations, to implement and to validate their various components. This team also defines

model experiments to run, co-ordinates their execution by the participating groups, and organises the sharing of model results.

2.3. Associate Scientists

The DRAKKAR project team promotes collaboration with Associate Scientists conducting researches complementary to the DRAKKAR objectives to enhance the scientific value of model developments, simulation outputs and to foster multidisciplinary studies. Associate scientists may also get DRAKKAR model configurations to carry out their own simulations. In that case, it is important that when possible, they co-ordinate their simulations with those carried-out with the project-team. An objective of DRAKKAR is to gather a community of competences and means to improve global eddy-permitting to eddy resolving models. Collaborating partners are thus expected to contribute to model refinement, in particular by additional, complementary sensitivity experiments. This includes the participation in experiments dedicated to the coordinated development. Associate scientists using DRAKKAR model configurations must commit themselves to not give model configurations to other groups. The DRAKKAR project team wants to control the distribution configurations to avoid their distribution on the grapevine.

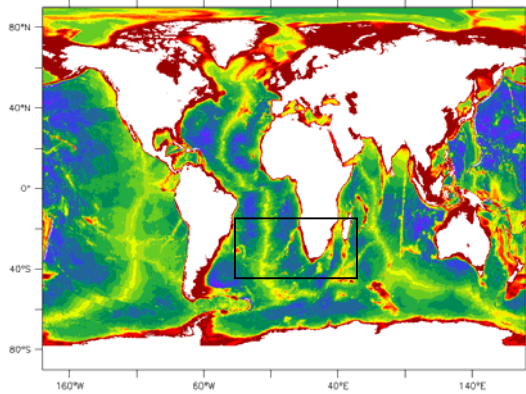
2.4. Cooperation with scientists outside the project

The DRAKKAR team is generally favourable to share model outputs and configurations with scientists outside the project. In case the scientific objectives of outside scientists overlap those of the project-team, a cooperation should be sought that favours complementarity of studies. Note that the group has no means dedicated to service outside the group, and technical support to transfer DRAKKAR configurations will be limited. Scientists using Drakkar model configurations must commit themselves to not give them to a third party. Major funding of DRAKKAR project comes from the MERCATOR consortium, and model configurations have been (and will continue to be) developed jointly with MERCATOR. Consequently, the team will not give model configurations to groups involved in activities directly related to operational or commercial oceanography. These groups will have to address such request directly to the MERCATOR consortium. Finally, it should be noted that DRAKKAR model configurations are not included in the NEMO distribution, but are using it. NEMO is freely available and is distributed by LOCEAN. Users of DRAKKAR configurations, as all NEMO users, must register at LOCEAN.

3. DRAKKAR model configurations

The various configuration of the ocean/sea-ice NEMO numerical model are schematically presented in the figure below. Advances in model performances achieved during the development of this hierarchy of configurations are described in a series of papers published or submitted (Barnier et al., 2006, Le Sommer et al., 2006, Penduff et al., 2006), and several reports (<http://www.ifremer.fr/lpo/drakkar/>).

a) Global Configurations

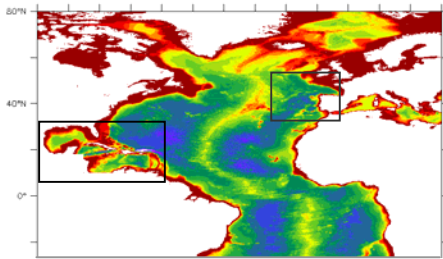


ORCA2: Global, coarse $\sim 2^\circ$ resolution, non eddy permitting configuration with sea-ice, $182 \times 140 \times 31$ grid pts, time step 9400 s. Operated at LOCEAN, IFM, and LEGI

ORCA05: Global, $1/2^\circ$ resolution, non eddy permitting configuration with sea-ice, $722 \times 511 \times 46$ grid pts, time step 2160 s. Developed in 2004. Operated at LOCEAN, IFM, and LEGI

ORCA025: Global, $1/4^\circ$ resolution, eddy permitting with sea ice, $1442 \times 1021 \times 46$ grid pts, time step 1440 s. Developed in 2005, Operated at LEGI, IFM-Geomar and MERCATOR-Ocean. IFM-Geomar is implementing a $1/12^\circ$ AGRIF refinement in the region of the Agulhas Retroflection region.

b) North-Atlantic/Nordic-Seas configurations (80°N – 30°S) driven at open boundaries by the global configurations



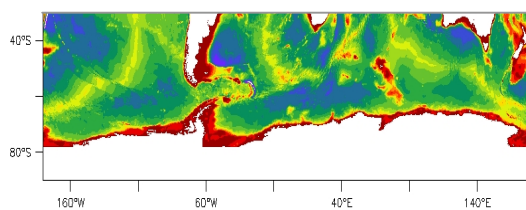
NATL4: $1/4^\circ$ resolution, eddy permitting, with sea-ice. Open boundaries, $486 \times 529 \times 46$ grid pts, time step 2400. Developed in 2004, it has the possibility of AGRIF grid refinement. Operated at LPO and LEGI.

AMEN: AGRIF refinement in NATL4 in the north east Atlantic: $1/12^\circ$ resolution, eddy resolving. AMEN has $383 \times 397 \times 64$ grid pts, time step 720s. Developed in 2006. Operated at LPO.

NATL12: $1/12^\circ$ resolution, eddy resolving, with sea-ice. Open boundaries, $1615 \times 1576 \times 64$ grid pts, time step 720s. Developed in 2006. Operated at LPO and MERCATOR-Ocean.

AGRIFMEX: NATL3 (similar to NATL4 at $1/3^\circ$ resolution, inherited from CLIPPER) with AGRIF refinement in the Caribbean/Gulf-of-Mexico (CARIB15): $1/15^\circ$ resolution, eddy resolving. NATL3 has $358 \times 361 \times 43$ grid pts, time step 1800 s. CARIB15 has $604 \times 399 \times 43$ grid pts, time step 600 s. Developed in 2006. Operated at CICESE and LEGI.

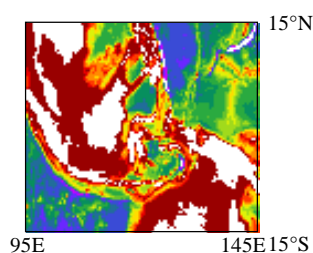
c) Southern Ocean configurations (30°S – 80°S) driven at open boundaries by the global configurations



PERIANT05: $1/2^\circ$ resolution, non eddy permitting, with sea-ice. Open boundary at 30°S , $722 \times 202 \times 46$ grid pts, time step 2400 s. Developed in 2006. Operated at LEGI.

PERIANT025: $1/4^\circ$ resolution, eddy permitting, with sea-ice. Open boundary at 30°S , $1442 \times 402 \times 46$ grid pts, time step 1440 s. Developed in 2007. Operated at LEGI.

d) Indonesian throughflow configuration (15°N-15°S) driven at open boundaries by the global configurations



ITF025: $1/4^\circ$ resolution, eddy permitting from 15°S - 15°N and 95°E - 145°E . Four open boundaries driven by ORCA025. $204 \times 210 \times 46$ grid pts, time step 2400 s. Developed in 2006. Operated at LOCEAN.

Figure 1: DRAKKAR Hierarchy of Model Configurations.

4. DRAKKAR Project: Report of Activity 2006

We present here a summary of research activities carried out in 2005 and 2006 by the DRAKKAR French Team (LEGI, LPO, LOCEAN and LSCE). A section of this report is written in French, because it is a paper submitted to the IDRIS newsletter, the news letter of the French National Computer Centre where all calculations presented here were performed. This paper presents a 47 year long experiment (1958-2004) carried out with the $1/4^\circ$ global configuration ORCA025-G70.

The report is organized as follows. The first part presents our efforts to improve the model configurations, numerical schemes, and forcing fields. The second part describes the long experiments with the $1/2^\circ$ model and the $1/4^\circ$ global model, and ongoing analysis. The third part presents the studies of the Southern Ocean, and the fourth our regional configurations. Finally, studies realized in collaboration with associated teams are summarized in the last section.

4.1. Improvement of DRAKKAR model configurations

4.1.1. Parameterisations

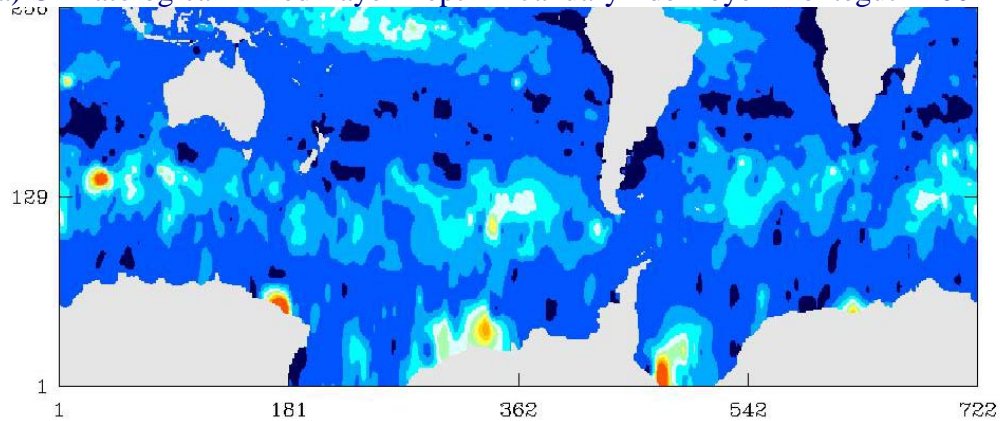
Experiments have been carried out in order to fix or reduce several identified deficiencies of the ORCA025 configuration in order to prepare the 50 year long inter-annual experiments. Four issues were addressed: The summer mixed layer, the freshwater runoff of the Amazon River, the overflows at major sills and straits, and the geometry of the strait of Torr s.

Mixed layer. The summer mixed layer was generally too shallow in model configurations based on NEMO. A modified *TKE* scheme (Madec, 2006) which accounts for (i) the effect of surface waves, (ii) an enhanced vertical penetration of the turbulent kinetic energy (*tke*), and (iii) includes a parameterisation of the effect of the Langmuir Cells on the vertical mixing have been tested in ORCA025. In this series of tests ORCA025 is run from rest during 4 years, driven by the CORE normal year atmospheric forcing. Results from two experiments are presented here: run G42 with standard *TKE* scheme, and run G43b with the modified *TKE* scheme in which the *tke* penetration is 7.5% of the wind energy. The mixed layer depth (*mld*) climatology of de Boyer Mont gut et al. (2004) is used to measure the impact of the new *TKE* scheme. The primary effect expected from the new *TKE* parameterisation is to increase the summer mixed layer depth, which is usually too shallow with respect to the climatology. In our calculations of the *mld*, we use the same temperature criterion as in the climatology (a 0.2°C temperature change).

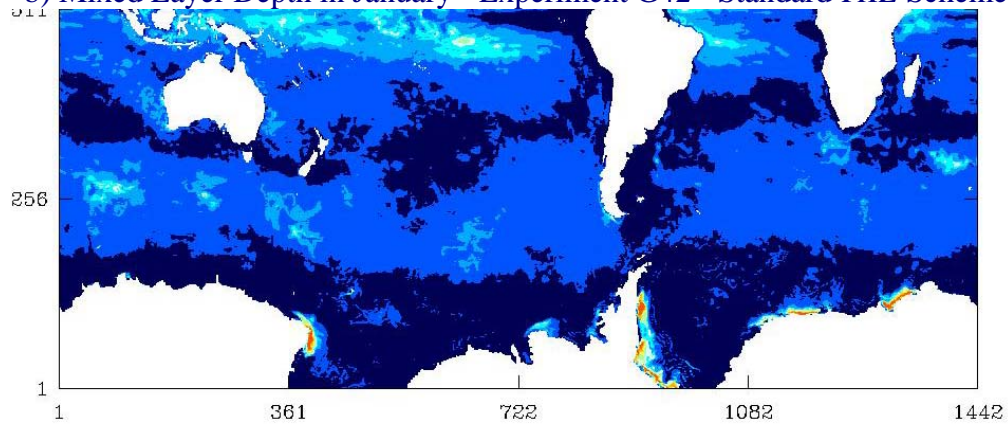
In the Southern ocean, the climatology indicates summer *mld* values of 60-100 m. (Fig 1a). With values of 40 m (Fig. 1b) the standard run (G42) significantly underestimate the *mld*. The run with the modified *TKE* (Fig. 1c) with a *mld* in the range 80-120 m is much closer to observations. In the northern hemisphere (no figure shown), the North-East Pacific is a region where the new *TKE* makes a noticeable difference. Climatology shows a wide band where *mld* is 40 m stretching from Bering Strait to California. The standard run G42 does not reproduce this feature with a *mld* which rarely exceeds 20 m. On the contrary, with the modified *TKE* scheme the model reproduces well the shape and amplitude of this feature. Similar result is observed in the North Atlantic, the new *TKE* scheme producing again a deeper summer *mld* than in the standard case. These improvements are found to be robust for every summer month in both hemispheres. However, we observed that the model *mld* produced by the modified *TKE* scheme often exceeded the observed values, suggesting that using a penetrating fraction of *tke* of 7.5% is slightly too strong. But setting the corresponding parameter to 0% (run G43a) produced too shallow *mld* as in the standard case. Our conclusion is that the new *TKE* scheme performs better

than the standard one, in particular in the Southern Ocean and we recommend to use a value of 5% for the fr_{emin} parameter which sets the vertical *eke* penetration.

a) Climatological Mixed Layer Depth in January - de Boyer Montégut - 2004



b) Mixed Layer Depth in January - Experiment G42 - Standard *TKE* Scheme



c) Mixed Layer Depth in January - Experiment G43b - Modified *TKE* Scheme

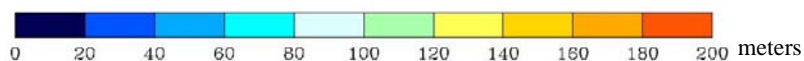
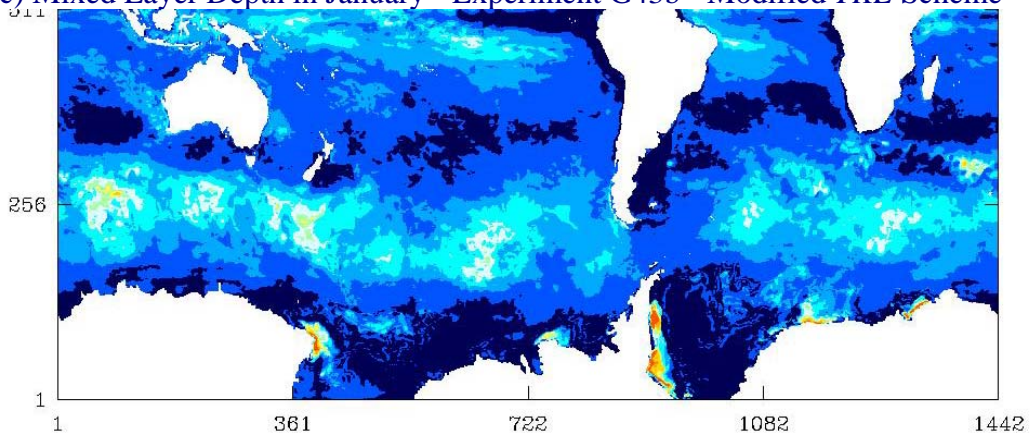


Figure 1: Summer mixed layer (January) in the Southern hemisphere from a) estimate from climatological hydrographic data by de Boyer Montégut (2004), b) by the model ORCA025 with the standard *TKE* vertical mixing scheme, and c) by the model ORCA025 with the new *TKE* vertical mixing scheme.

Amazon river runoff : the strong runoff of the Amazon river was found not to spread out enough off shore the river outlet, generating an unrealistic, very fresh coastal current along the Brazil-Guyana Coast, feeding the Caribbean Sea with too fresh upper waters. An analysis of this particular case have been realized and modification of the runoff distribution at the outlet have been proposed (run G45b).

Overflow parametrization : All DRAKKAR simulations carried out in 2005 showed deficiencies in the representation of deep water overflows, which occur mainly between the Norwegian Sea and the North Atlantic (Denmark Strait and Faroes Bank Channel, hereafter respectively named DS and FBC), the Mediteranean Sea and the Atlantic (Gibraltar Strait, hereafter GIB) and between the Red Sea and the Gulf of Aden (Bab-el-Mandeb strait, hereafter BEM). Sensitivity experiments have been carried out first with the idealised DOME configuration, then with the NATL4 configuration (for a fine tuning in DS, FBC and GI), to find modifications of the bottom topography, and for fine tuning of locally enhanced bottom friction and parameters of the diffusive and advective bottom boundary layer (BBL).

First, the numerical code of the advective BBL has been modified to run with the Partial Step topography. Second, a series of tests with the idealised DOME configuration demonstrated that increasing bottom friction was significantly contributing to bring overflow waters at greater (and more realistic) depths. However, tests with NATL4 demonstrated that this effect was much more limited in a realistic configuration.

Third a modification of the topography of the sills which would optimise the effect of the advective BBL has been searched. Using the DOME configuration, we demonstrated that the advective BBL is the most efficient on the first topographic step. The DOME configuration is a 1200 km long, and 300 km wide, east-west channel (Figure 2a). It is shallow to the north and deep to the south, depth increasing linearly from north to south. The flow is linearly stratified. A flow of water which density is the bottom density is injected at 600 m depth in a narrow north-south channel at the north-east corner. The topographic slope in this narrow channel has one of the profiles shown in Fig. 2b. The dense water flows down-slope and westward, and tends to form a vein of dense fluid at some depth. A passive tracer of concentration one is injected in the dense water at the entrance of the narrow channel. The tracer concentration at the near bottom level is taken as the dense water overflow.

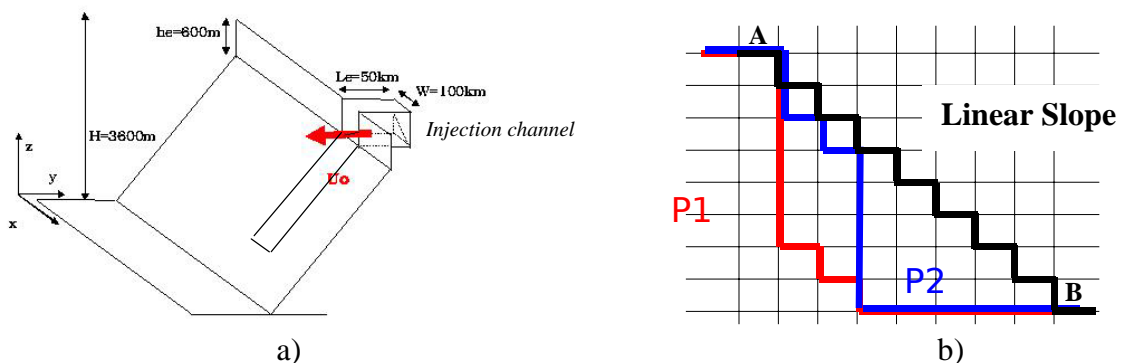


Figure 2: Schematic representation of a) the DOME configuration and b) the various topographic profiles tested for the injection channel in the DOME configuration. The cliff profile is P in red. A (and B) are the top (and the bottom) of the dense water injection channel. The study aims to quantify the impact the different profiles have on the descent of dense water (i. e. passive tracer).

Among the 3 different topographic profiles shown in Figure 2, the profile which has the greater topographic jump (profile P1, the cliff profile thereafter) is the one insuring the highest concentration of a passive tracer from A to B, but only when associated to the advective BBL (Fig. 3).

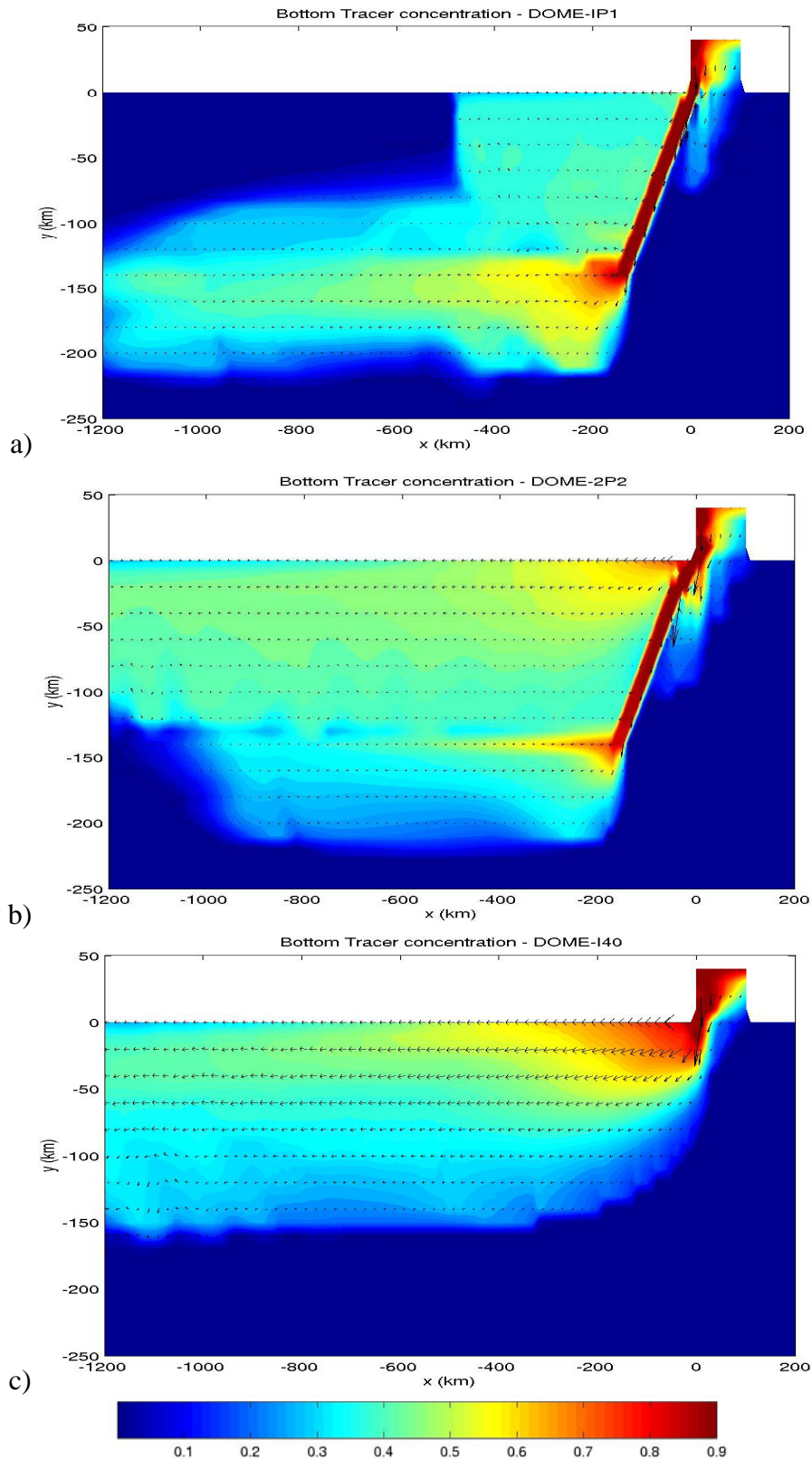


Figure 3: Concentration of passive tracer(colours) near the bottom after 60 days in 3 different DOME runs with advective BBL, a) with the "cliff" profile P1, b) with profile P2 and c) with the linear profile. It is the cliff profile P1 associated with the advective BBL which has the highest concentration of tracer at the exit of the channel at $y = -140$ km. The other profile P2 has a lesser tracer concentration at depth and shows a strong leakage at the upper part of the channel. With a linear slope, no dense fluid is found at the depth corresponding at $y = -140$ km. Arrows show current velocity.

The modification of ORCA025 bottom topography at DS, FBC, GIB and BEM has been inspired by the above DOME results. The bathymetry of those straits have been modified such that the greatest topographic jump occurs at the first grid point after the sill (Figure 4 for the Denmark strait). The results are very positive regarding the depth reached by the overflow waters. However, this solution was found to under-mix the Mediterranean outflow waters which were much too warm and salty. Relaxation to climatological values was thus implemented at the outlet of the sill for the ORCA025-G70 experiment (1958-2007). After viewing the results of run G70 (see below), the good behaviour at GIB suggests that a similar relaxation should also be used at BEM.

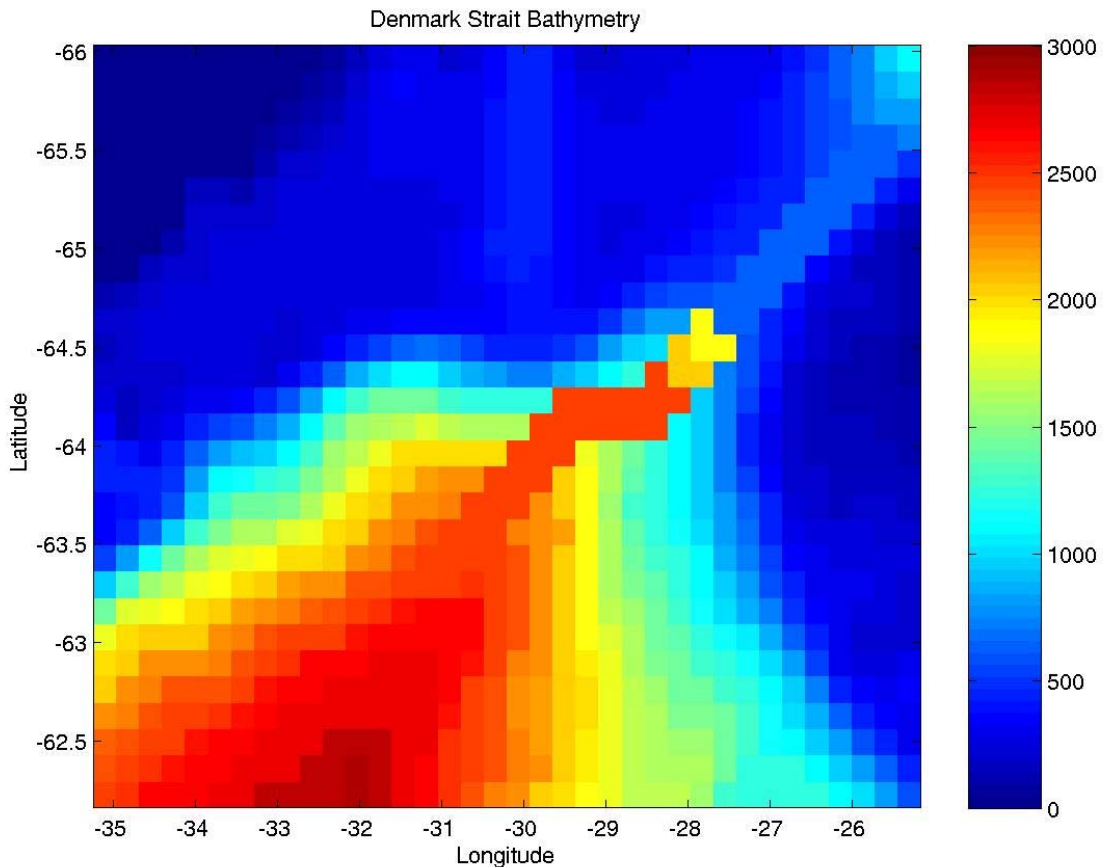


Figure 4: Denmark Strait bottom topography (in meters) in ORCA025-G70. The channel connecting the Nordic Seas to the North Atlantic is characterised by a jump at the sill from nearly 600 m to 1800 m (the yellow colour at 64.5°N, 27.6°W).

Opening Torr s Strait : The tuning of the bathymetry in the Indonesian through-flow area first led to the closing of the Torr s Strait, in order to reduce the water transport through it. This drastic solution was not fully satisfactory because of the lack of diffusive transport between the Pacific Ocean and the Arafura Sea is questionable. We decided to open the strait, including 2 small islands to mimic the effect of very shallow areas, and using locally enhanced bottom friction (factor of 50) in order to slow down the flow as much as possible. This solution proved to be rather satisfactory (runs G44, G45 and G45b).

Definition of sea-ice model parameters: We used the $1/2^\circ$ southern ocean configuration PERIANT05 to tune the sea-ice parameters in the Antarctic. The accretion parameter for sea-ice proved to be crucial regarding ice thickness. Parameters values used in the run ORCA025-G70 are issued from these experiments (Molines et al., 2006).

4.1.2. Momentum advection

A series of simulations with the NATL4 configuration have been carried out to understand the influence of momentum advection schemes on mean currents and current-topography interactions. It was found that near-bottom grid-scale velocity irregularities play a major role. The first DRAKKAR global simulations at $1/4^\circ$ have shown that the use of an enstrophy-and-energy-conserving momentum advection scheme substantially reduces widespread biases of mean currents at the surface (Barnier et al., 2006) and at depth (Penduff et al., 2006). We have investigated the origin of these improvements (Lesommer et al., 2006). A series of sensitivity simulations with different momentum advection schemes is performed with the North Atlantic $1/4^\circ$ DRAKKAR model NATL4. Three second order momentum advection schemes conserving respectively enstrophy (*ens*), energy (*efx*) and both quantities (*een*) are tested and their impact on the model solution are compared. The mean kinetic energy vertical profile is found to change within up to 10% depending on the chosen scheme. This sensitivity is maximum in bottom layers. The analysis of the vorticity tendency due to horizontal momentum advection reveals that the three schemes differ mostly in bottom layers indeed. The average magnitude of this term is enhanced with scheme *efx* and reduced with scheme *een*. These differences are found to be consistent with the instantaneous tendency of each scheme. In addition, we show that these differences are related to the irregularity (i.e. non-smoothness of the gradients) of the velocity field, which is enhanced in bottom layers. We conclude that the model solution is crucially dependent on the ability of the momentum advection scheme to handle under-resolved flows close to the bottom topography. This work emphasizes the critical influence of current-topography interactions in eddy-active regions on mean current features such as the position of the North-Atlantic current, the Gulf Stream separation, or the Zapala Anticyclone in the Argentine basin.

4.1.3. Atmospheric forcing: Definition of DFS3

A series of studies have been conducted to produce a forcing function which correct the major biases and drifts noticed in run ORC05-G50. The only equivalent forcing data set available is the ECMWF reanalysis ERA40. Radiative fluxes (downward short wave and long wave) from ERA40 show a strong trend over the whole period (Brodeau et al., 2006), and they were discarded. We decided to retain CORE radiation which is a satellite product (ISCCP). We compared the turbulent fluxes of CORE and ERA40. The basic variables (wind speed, air temperature and air humidity) are rather different between data sets (Figure 5 and Figure 6). CORE winds are always stronger, and are suspected to be too strong since they are also stronger than ERS satellite winds.

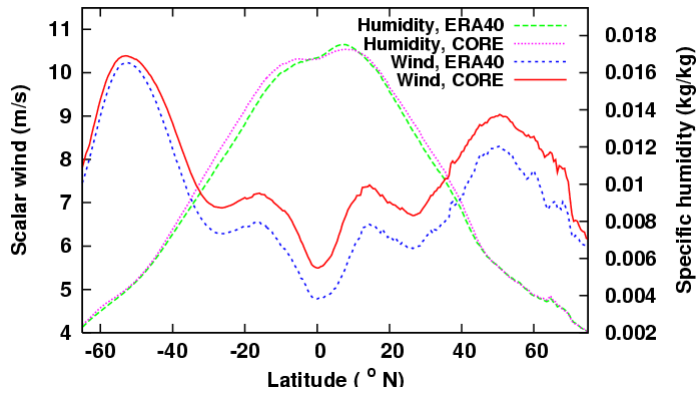


Figure 5: Latitudinal distribution of the zonally averaged 10m wind speed and 10m air humidity in ERA40 and CORE data sets. The 1958-2000 mean is plotted. CORE wind is significantly greater. Air in ERA40 is generally dryer than in CORE excepted in the 0°N-10°N equatorial band.

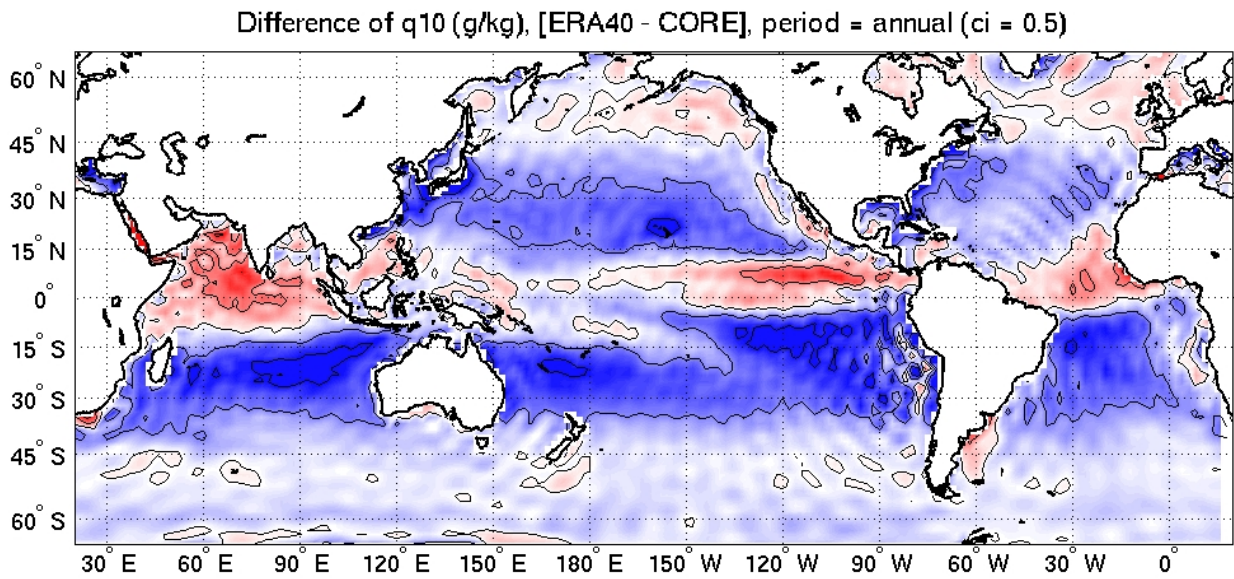


Figure 6: Mean difference in 10m air humidity between ERA40 and CORE. This difference is calculated over the period 1958-2000. Positive (negative) values in red (blue) areas indicate moister (drier) air in ERA40. We expect a significant reduction of the latent heat flux in the tropics with ERA40 due to weaker winds and moister air. Stronger evaporation is expected in subtropical gyres and the ACC, significantly dryer in ERA40, which amplitude might be however limited by weaker wind speed. Note that the "wiggles" are introduced by CORE, ERA40 fields being significantly more regular. Contour interval is 0.5 g/kg.

Air is dryer in ERA40 excepted in the band 0°N-10°N. Regarding air temperature (Figure 7), EA40 is warmer between 30°S-30°N, and in north-eastern Pacific and Atlantic Oceans. At subpolar latitudes in the northern hemisphere (no figure shown), air in ERA40 is slightly warmer than in CORE (about 0.5°C), but is significantly colder in winter (1 to 3°C in the Labrador Sea for example). Thus we expect more active deep convection in the North Atlantic with this data set. In the Arctic (Figure 8), ERA40 temperature is higher (by 2°C or 3°C) in all seasons. Interannual variability is very consistent between both data sets over the whole 1958-2001 period.

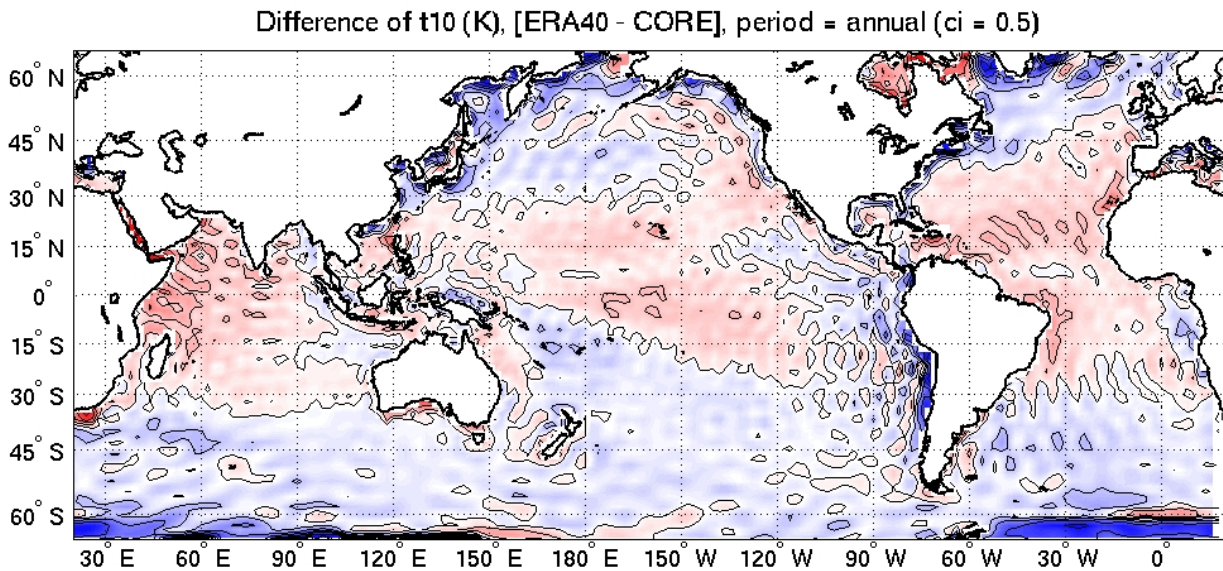


Figure 7: Mean difference in 10m air temperature between ERA40 and CORE. This difference is calculated over the period 1958-2000. Positive (negative) values in red (blue) areas indicate warmer (colder) air in ERA40. Note that the "wiggles" are introduced by CORE, ERA40 fields being significantly more regular. Contour interval is 0.5°C.

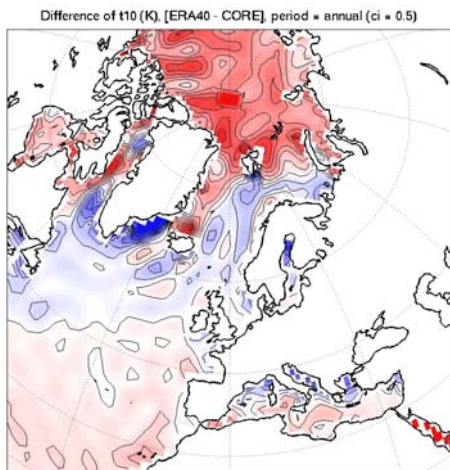


Figure 8: Difference in 10m air temperature between ERA and CORE in the Arctic. Positive (negative values) in red (blue) indicate warmer (colder) air in ERA40. Contour interval is 0.5°C. In area covered by sea-ice, air in ERA40 is significantly warmer, suggesting that ice thickness might be less in a run driven by this data set.

Our analysis of the freshening of the surface ocean in run ORCA05-G50 identified precipitation as an important contributor at mid and high latitudes in the northern hemisphere. We decided to apply a correction to the CORE precipitation between 30°S to the North Pole. CORE precipitation are derived from the GXGXS precipitation data set (Fig. 9), but a correction was applied which increased the amount of rainfall over the ocean by 0.3 to 0.5 mm/day in zonal average (Fig. 10). The reader is invited to see Large and Yeager (2004) for the justification of the correction. Analysis of simulation G50 suggests that the correction is reasonable except beyond 30°N, so we decided to use the standard GXGXS precipitation field between 90°N and 30°N and to keep the CORE values from 30°N to 80°S (Figure 10). This blended data set is referred to as DPS3 (Drakkar Precipitation Set #3).

GXGXS precipitation dataset

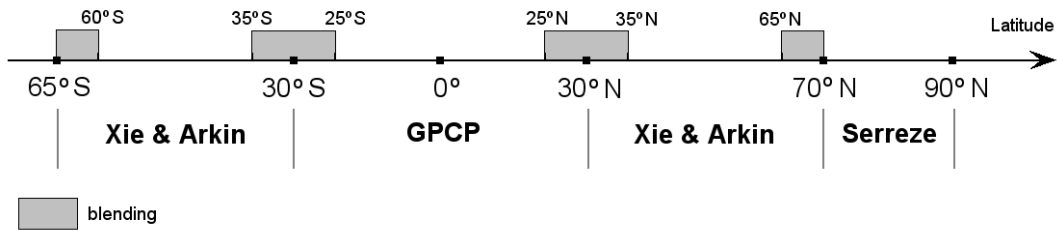


Figure 9: GXGXS precipitation data set: it is a blending of various precipitation estimates, which largely rely on satellite estimates. The study of Béranger et al. (2006) identified Xie&Arkin (also named CMAP) and GPCP estimates as the most reliable estimates among 20 different global precipitation fields to drive an ocean model.

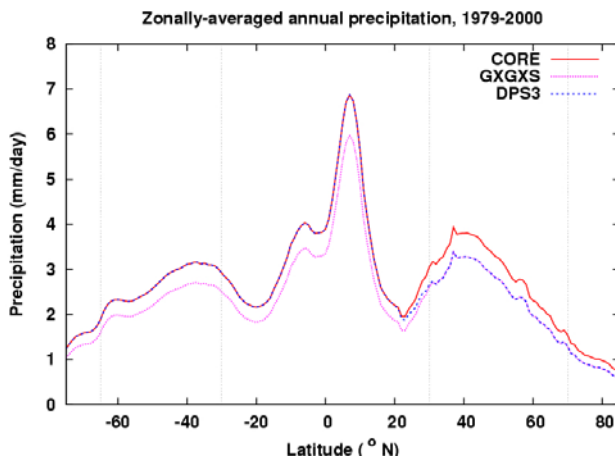


Figure 10: Latitudinal distribution of zonally averaged precipitation in the CORE and GXGXS data set. DPS3 (DRAKKAR Precipitation Set #3), retained for the hybrid DRAKKAR Forcing Set #3 is a blend of GXGXS from 90°N to 30°N and CORE from 30°N to 80°S.

DRAKKAR Forcing Set #3 (DFS3): From the above analysis, we defined a new set of atmospheric forcing variables, referred to as DFS3. It comprises :

- daily downward shortwave and lonwave radiation from CORE (ISCCP satellite product)
- PS3 monthly precipitation (CORE corrected by GXGXS northward beyond 30°N)
- 6 hourly wind vector (10 m), air temperature (10 m), air humidity (10 m) from ERA40 between 1958 and 2001, and from ECMWF operational analysis from 2002 to 2004.
- a correction for the katabatic winds in Antarctica (see below)
- monthly climatology of river runoff (from MERCATOR-Ocean operational center).

A series of experiments using DRAKKAR global configurations at 2° and 1/2° and have been used to evaluate DFS3, and confirmed that this forcing set produces more intense convection at high latitude, reduces significantly the freshening of the upper ocean and produces a stronger overturning. DFS3 was retained for the next DRAKKAR 50 year global experiment at 1/4° resolution, run ORCA025-G70.

4.2. Long simulations of the global variability

4.2.1. Run ORCA05-G50 : a 56 year long simulation from 1949 to 2004

This run is the first interannual experiment of the 1/2° global DRAKKAR configuration ORCA05 driven by the CORE forcing set (Large et Yeager, 2004) with 6 hourly forcing for turbulent fluxes. Although the interannual CORE forcing starts in 1958, the run was spun-up in 1949 because transient tracers begin to enter the ocean in the early 1950s. Therefore, the run starts January 1st 1949. CFC is started after 1 year (i.e. 01/01/1950), and Bomb-C14 after 6

years (01/01/1955). From 1949 to 1958, the model is driven with the forcing of year 1958 made periodic and repeated cyclically. Then from 01/01/1959 to the end of 2004, the interannual forcing is used. This run departs from the previous DRAKKAR runs (G0x to G4x series) in many aspects. It has the following characteristics:

- modified *TKE* scheme, with a 5% penetrating fraction of *tke* as recommended from our sensitivity studies
- open Torr s Strait with enhanced bottom friction (x50) and 2 islands in the strait
- modified bathymetry at the various straits, (overflow regions adapted to help BBL work)
- new runoffs provided by Mercator (Romain Bourdall  Badie, Nov. 2005)
- modified Sea-ice parameters (different from standard values)
- initial state for sea-ice deduced from January of the year 10 of run G45b
- enhanced SSS restoring in the Red Sea
- restoring to climatological SSS with a time scale of 36 days, except under sea-ice where no relaxation is applied, as in the standard DRAKKAR runs.

To follow the evolution on a year to year basis of the main characteristics of the model solution, an original monitoring system of the model integration has been developed. It produces time-series of relevant model variables like temperature and salinity drifts, MOC at given latitudes, depth averaged transport through major straits (Fig. 11), overflows at DS, FBC, GIB, etc., and many other indexes.

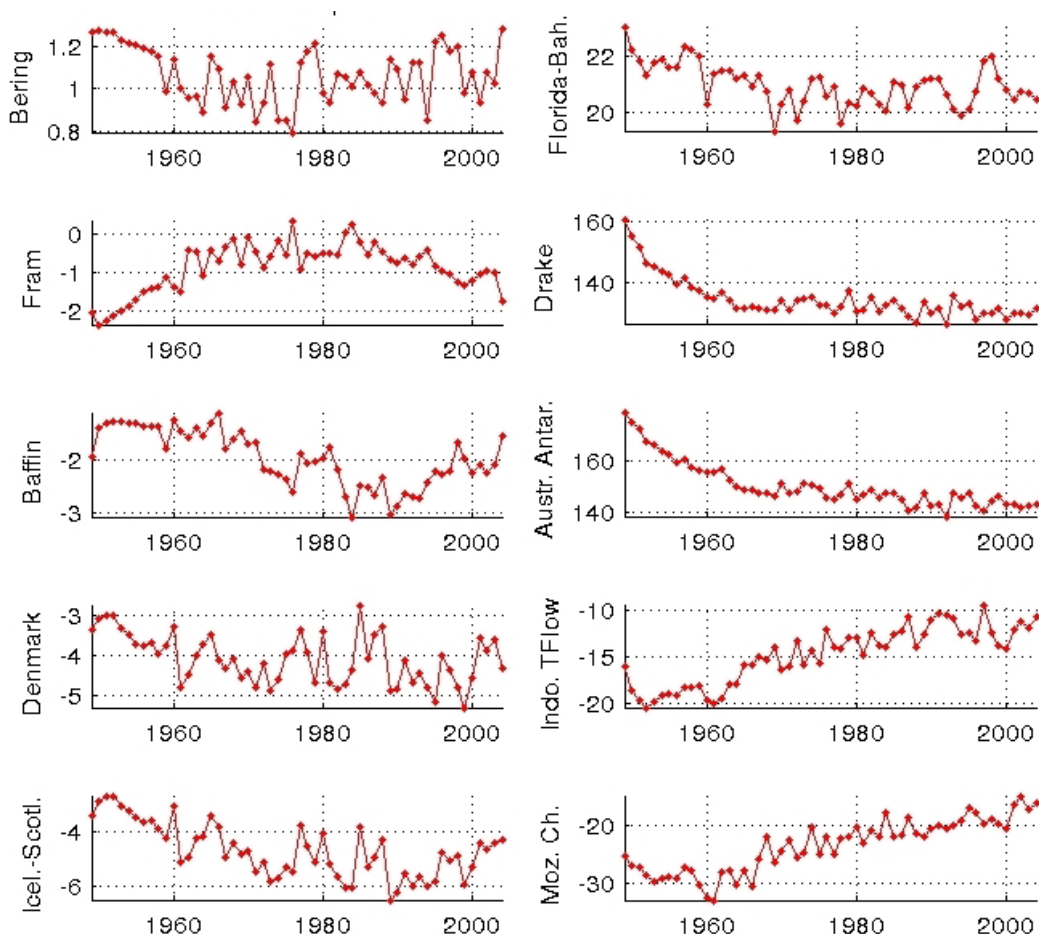


Figure 11: Run ORCA05-G50: Monitoring of the annual mean depth integrated transport (in Sv) across 10 major straits.

The analysis of the variability simulated by this experiment is presently on going and is compared to observations. Already, it has been established that the model simulates rather well the variability of the SST in the equatorial Pacific and El-Nino events (Fig. 12 & Fig. 13).

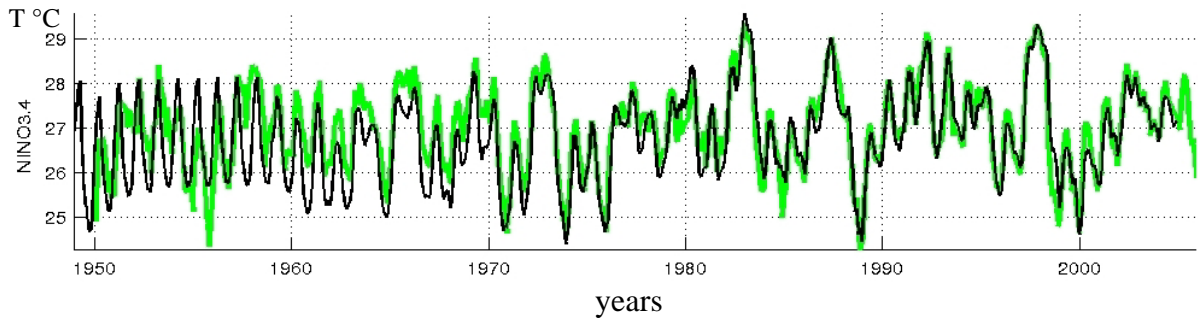


Figure 12. SST evolution in zone Nino3.4 (central equatorial Pacific) between 1949 and 2004 as simulated by ORCA05-G50 (CORE forcing). The black line is the model and the green line the observation. Passed the spin-up phase (1949-1958) when the model is driven by a repeated periodic annual forcing, one notices the remarkably good agreement between simulated and observed SST (correlation is 0.95 and bias less than 0.22°C).

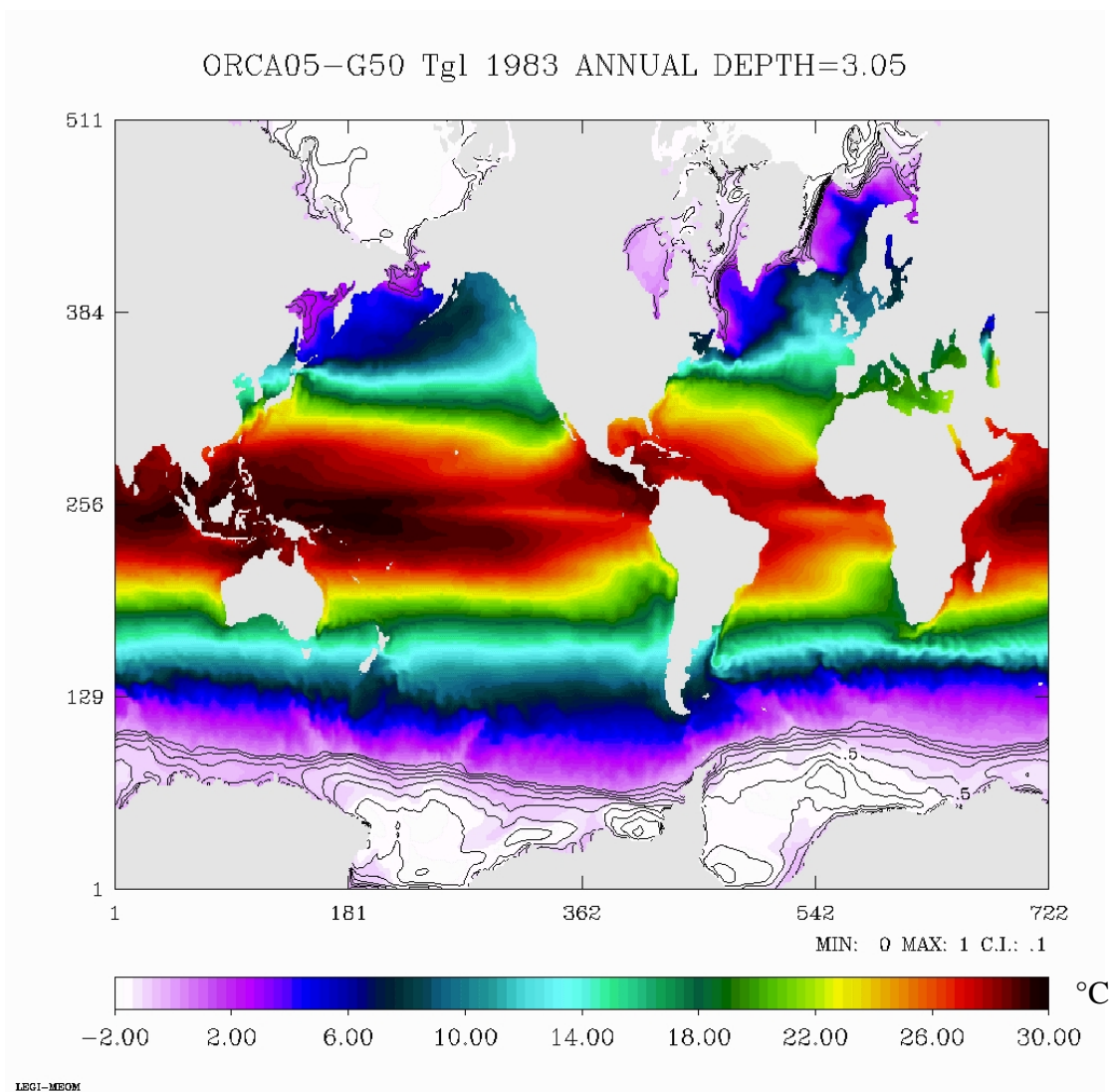


Figure 13: Annual mean SST (°C in colour) and sea-ice thickness (contour lines in meters) in 1983 (year of a strong El-Nino). Notice the warm water along Central America.

However, this experiment being the first interannual experiment using the CORE forcing, our priority was to investigate the amplitude of the meridional circulation and model drifts in order to identify flaws in the forcing which could be improved for the next simulations to come. This analysis shows a strong rise of the global sea level (Fig . 14a) going with a global freshening of the ocean at high latitudes, principally in its upper layers (Fig 14b). Deep convection in the Nordic Seas and the Labrador Sea is generally weak, and the amplitude of the Meridional Overturning Cell (MOC) is below 12 Sv in annual mean. We also noticed a progressive decrease of the overflow waters from the GIN Seas which density shifted from $\sigma_0 = 27.8$ to $\sigma_0 = 27.6$ (Fig. 14c).

The major reason for this is an excess of freshwater in the CORE forcing at high latitudes. The results motivated the construction of an hybrid atmospheric forcing combining satellite, CORE and ERA40 variables, the DRAKKAR Forcing Set # (DFS3), described in the next section.

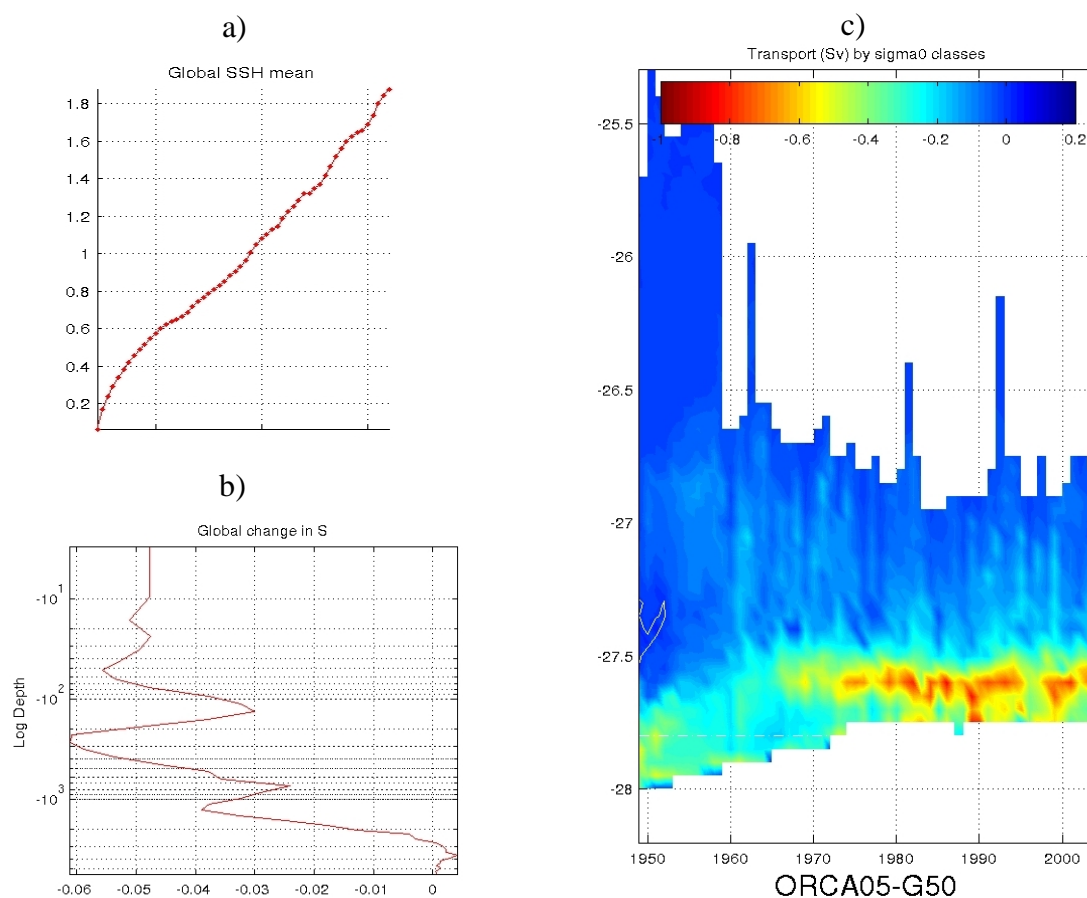


Figure148. Monitoring of ORCA05-G50. a) Evolution of the global mean sea level. The increase is 1.9 meters over 56 years. b) Horizontally averaged Salinity: difference between initial conditions and 2004 as a function of depth. Waters above 3000 m have freshened during the run, especially in the top 100 meters. c) Volume transport (in Sv) by density classes (σ_0) across Denmark Strait (negative values indicate a flow from the GIN Seas into the Atlantic). As time integration proceeds, the density of overflow water decreases. In 1972, overflow waters are always lighter than 27.8 (the white dashed line). In 1974, most overflow waters have a density of 27.6, but significant interannual variability is noticeable.

4.2.2. ORCA025-G70: a 47 year long simulation from 1958 to 2004

This run is the first interannual experiment carried out with the $1/4^\circ$ global DRAKKAR configuration ORCA025. It is driven by the DFS3 forcing described above, which differs from the CORE forcing used previously by the use of ERA40 6 hourly variables in the calculation of the turbulent fluxes, a reduction of precipitation north of 30°N and a correction for the katabatic winds in Antarctica. Differently to the previous run ORCA05-G50, we applied a relaxation to SSS climatology under sea-ice. The model starts from rest on January 1st 1958, with initial conditions from Levitus (1994) climatology for T,S. CFC and BombC14 calculation is started after one year of spin-up on January 1st 1959 with as initial condition the concentration from run ORCA05-G50 at this date. Details about the set-up of this experiment are given in a report by Molines et al. (2006). The run is presently in year 2003. Most flaws noticed in the previous run have been significantly corrected. The *ssh* trend, as well as the tri-dimensional T and S trends, has been considerably reduced, deep convection is strong in winter in the GIN and Labrador Seas, and the maximum amplitude of the MOC remains around 16/17 Sv during the duration of the experiment. We also notice the good depth of the Mediterranean water outflow, thanks to the use of a local relaxation, and the persistence of overflow waters denser than $\sigma_0 = 27.8$ in Denmark Strait and the Faroe Channel (Figure 15).

A overview of this simulation will be published (in French, Molines et al., 2006) in the next newsletter of the IDRIS computational centre where all model calculations mentioned in this report have been performed. The content of this newsletter is attached at the end of this report.

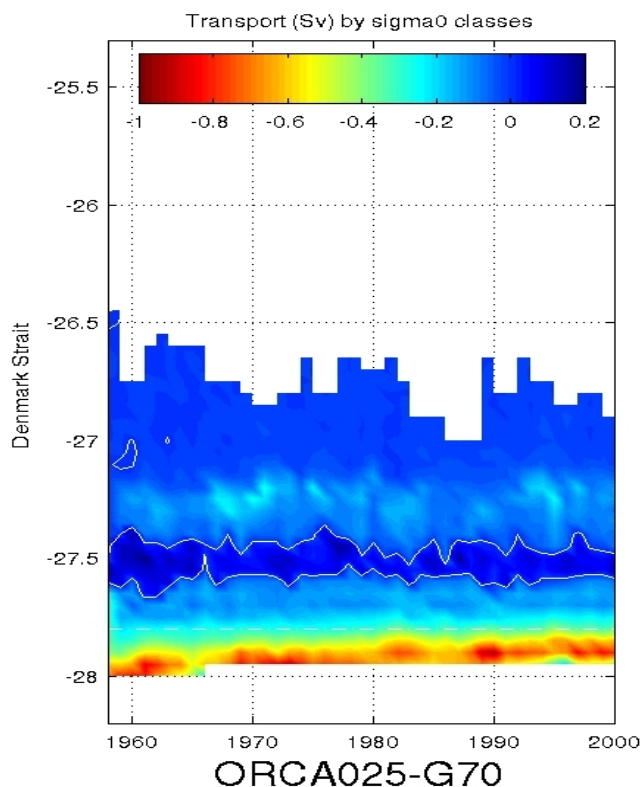


Figure 15. Monitoring of ORCA025-G70. Volume transport (in Sv) by density classes (σ_0) across Denmark Strait (negative values indicate a flow from the GIN Seas into the Atlantic). As time integration proceeds, the density of overflow waters slightly decreases, but remains denser than 27.8 (the white dashed line). Significant inter-annual variability is noticeable in the amplitude of the overflow.

The ERA40 reanalysis stops in early 2002. The first part of the ORCA025-G70 has been carried out until the end of 2001, and we have switched to a new forcing set for years 2002-2004. The CORE radiative fluxes and precipitations are still used through the end of 2004. The other forcing variables are taken from the ECMWF operational analysis (ECMWF hereafter) provided through a partnership with MERCATOR-Ocean. We have verified a good continuity of the wind, and to a lesser degree air temperature between the two datasets. On the other hand, the air humidity differs considerably between ERA40 and ECMWF, operational analysis producing

significantly dryer air (0.3 g/kg) in the 20°N-20°S latitude band. We have reasons to believe that the ECMWF humidity is more realistic (ERA40 is known to be biased high), so we have applied no correction. Users of the ORCA025-G70 experiments are warned that this discontinuity in the forcing may result in spurious interannual variability between 2001 and 2002 in the tropics.

4.2.3. Analysis of model simulations with regard to observations

Runs ORCA05-G50 and ORCA025-G70 are presently being analysed. An important effort is carried out at LEGI (T. Penuff and M. Juza) to confront these model results to observations over the same period. Tools have been developed which permit to collocate model output with observation of the ENACT/ENSEMBLES (including CTDs, TAO moorings, XBTs and ARGO data) and AVISO data bases. This permit to carry out collocated model/observation comparisons with advanced statistical methods. This activity is just starting, and an example is shown below (Fig. 16).

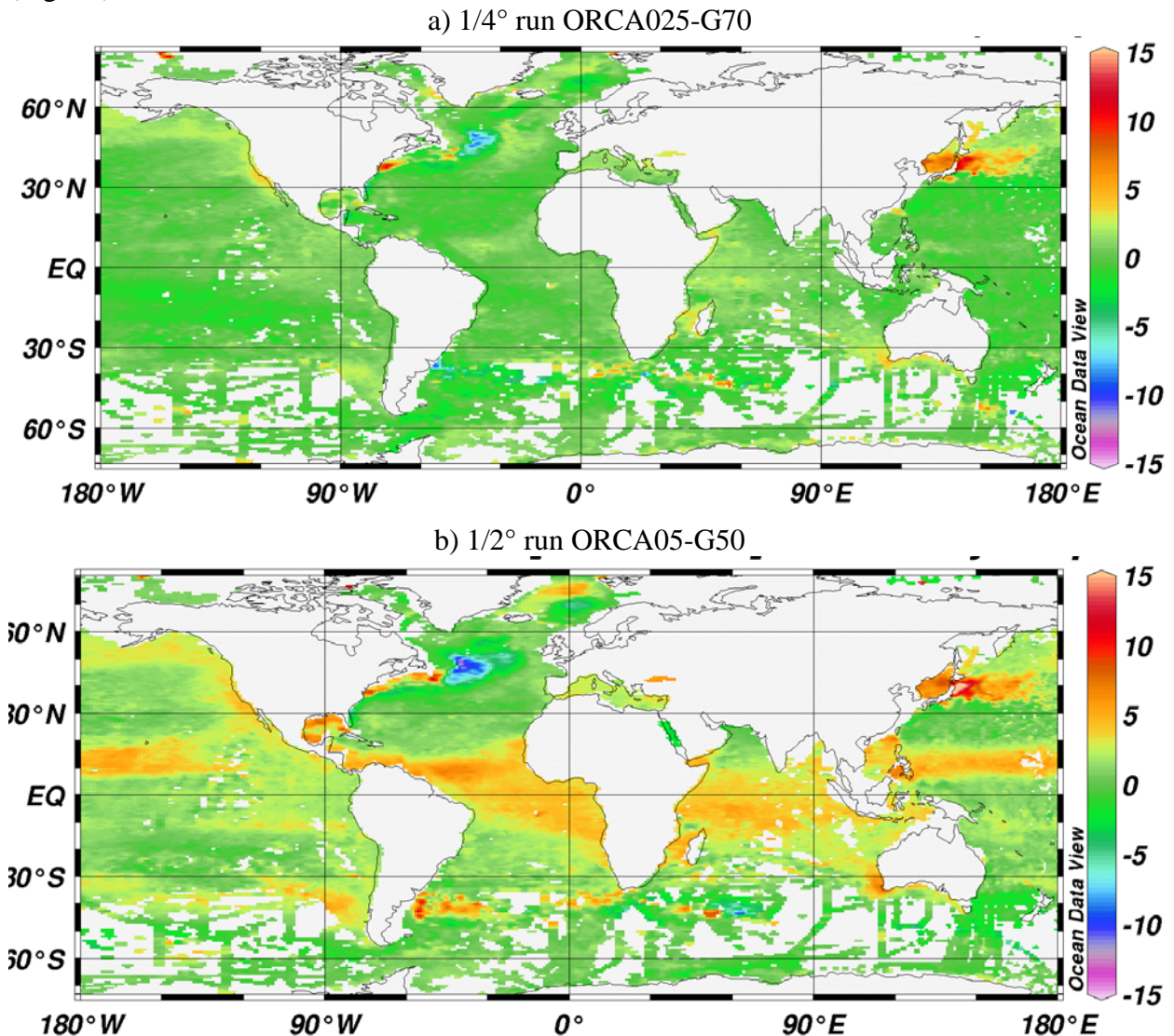


Figure 16: Difference in ocean heat content integrated from 50 m to 450 m between collocated model and hydrography during the period 1980-1995. a) The model is the 1/4° ORCA025-G70 experiments, and b) the model is the 1/2° ORCA05-G50 experiment. Despite significant biases remaining in the Kuroshio and the Gulf Stream/NAC regions, the integrated heat content is significantly closer to observations in the 1/4° simulation.

4.3 Dynamics of the Southern Ocean

Our studies in the Southern ocean have started at the beginning of 2005 with the PhD of Pierre Mathiot, in collaboration between LEGI and LGGE, with the objective of studying the effect of the katabatic winds on the formation of sea-ice and water masses. A second project, started in 2005 in collaboration Australian colleagues, is aimed at understanding better the dynamics of the Antarctic circumpolar current and the variability of water mass formation in the Southern ocean. The latter was also the central theme of the project presented by Julien le Sommer at CNRS in 2006 (Julien is now CNRS scientist at LEGI, currently on leave at the University of New South Wales).

4.3.1. Correction for Katabatic Winds

It has been shown that in the Antarctic, ERA40 has katabatic winds of small amplitude (Mathiot, 2005). A downscaling of ERA40 winds has been performed by H. Gallée (LGGE) with a regional model of the Antarctic atmosphere (MAR model) over a 10 year period (1980-1989). The comparison of ERA40 and MAR winds at the coast around the continent showed that MAR winds have greater amplitude. A correction factor, define by the mean slope of the scatter plot of Fig. 17a, has been applied to correct ERA40 winds near the coast (Fig. 17b, the details of the correction method is not given here, PhD thesis of P. Mathiot).

Several 10 year long simulations were carried out with the $1/2^\circ$ Southern Ocean DRAKKAR configuration with both corrected and uncorrected ERA40 winds. They show (Fig.18) that the correction of katabatic winds increases the amplitude and extent of coastal polynia (thinner sea-ice) and that colder and saltier waters are produced around Antarctica, which T,S properties compare better with observations.

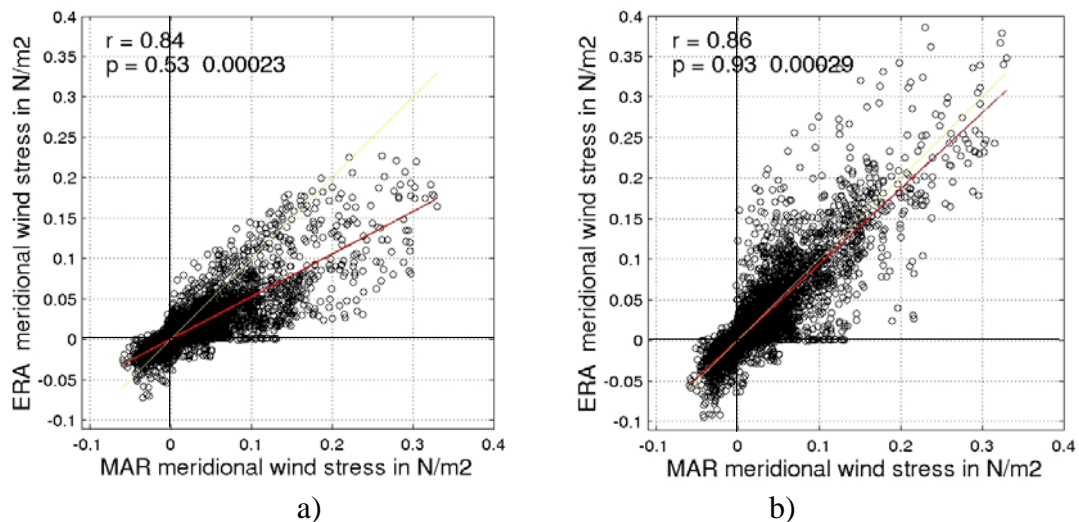


Figure 17: Scatter plots comparing the meridional wind component of MAR and ERA40 at the coast around the Antarctic continent (the comparison of the zonal component, not shown, gives very similar results). a) The raw fields are compared. Correlation ($r = 0.84$) is rather good, indicating good consistency of wind direction between data sets. In term of amplitude, ERA40 winds are generally weaker, by almost a factor of 2 in average. b) Comparison after correction of ERA40 winds. Correlation ($r = 0.86$) is slightly increased, and the amplitude bias is now less than 10%.

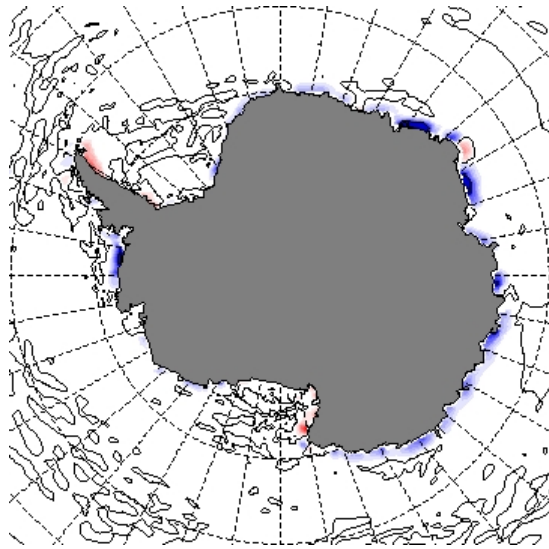


Figure 18: Difference in the time mean zonal wind stress between corrected ERA40 and uncorrected ERA40. Blue areas indicate strong eastward winds. The picture is obtained with the meridional component indicate stronger northward wind in these areas in corrected ERA40. These regions are regions of known katabatic winds. The correction vanishes offshore over about a 100 km.

4.3.2. Antarctic circumpolar ocean dynamics

This work is based on the global $1/4^\circ$ DRAKKAR model and has been initiated during a 4 month stay of A.M. Treguier in Australia from October 2005 to March 2006. It is a collaboration with M. England (University of New South Wales, Sydney) and S. Rintoul (CSIRO, Hobart), financed by a PAI (FAST-DEST program) and the ARC (Australian research council).

The Antarctic circumpolar current (ACC) which flows around Antarctica without encountering continental barriers, is the prominent feature of the Southern Ocean. Due to its geometry, the ACC has often been compared with the atmospheric jet stream and studied in a "zonal mean" framework. The ACC path is strongly influenced by continental masses, however. This is shown in Fig.19 where the ACC extension is indicated by black contours (time-mean barotropic streamlines). Ivchenko et al (1996) were the first to study the ACC dynamics following streamlines, and they showed that zonal means underestimate the contribution of transient eddies to the dynamics. All recent theories of the ACC are based on an analysis following streamlines (for example, Marshall et Radko, 2003). Those theories are based on a simplified density equation: the purpose of our work is to assess the validity of those simplifications in the ORCA025 model. One key contribution to the density balance is the atmospheric forcing (Fig 19a). In the model the ACC gains buoyancy (average negative flux in Fig.19) because the freshwater input dominates the cooling contribution. There is a large cooling region in the south west Pacific that coincides with deep surface mixed layers (Fig.19b).

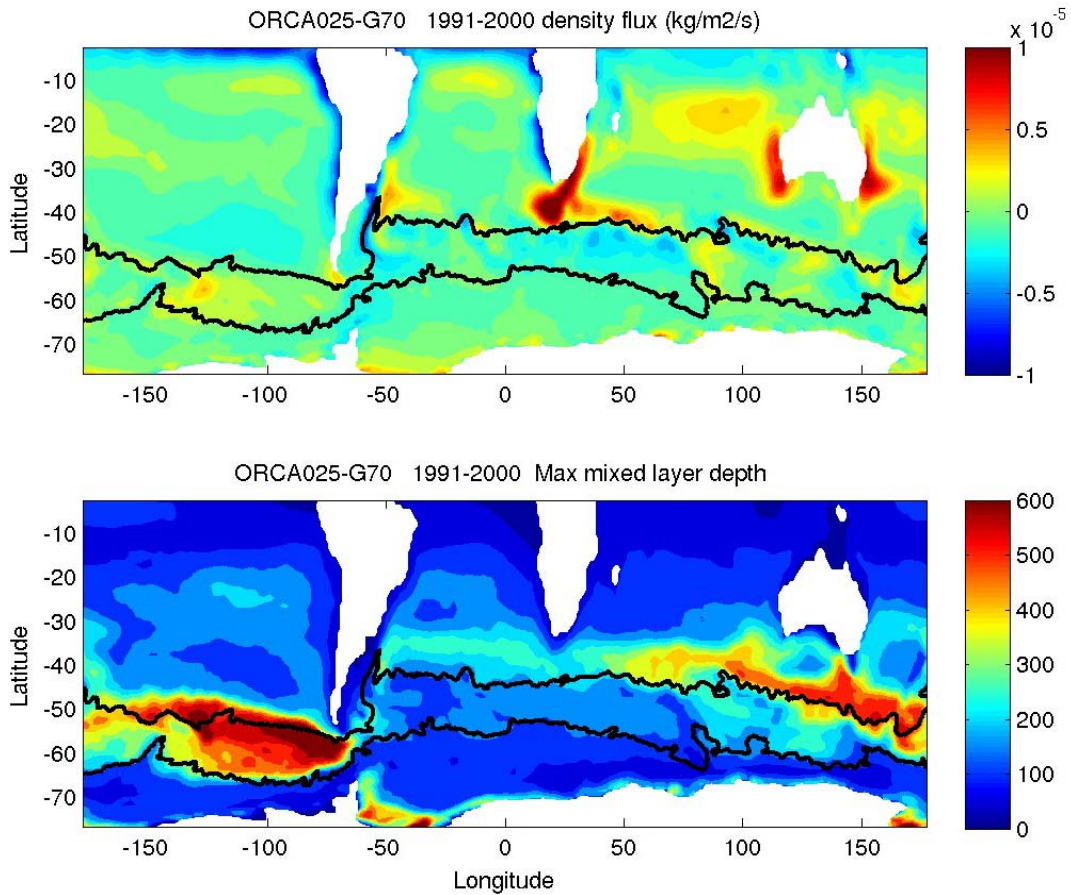


Figure 19: Density surface flux (top) and maximal mixed layer depth (bottom) for the global $1/4^\circ$ DRAKKAR model, years 1991 to 2000. The ACC is defined by the two black contours (barotropic streamfunction lines going through Drake Passage).

Just considering the streamline geometry suggests a more complex equilibrium than assumed by theories. All streamlines "climb" onto continental slopes like the Falklands or the Kerguelen islands, and all cross regions of deep mixed layers. It is thus impossible to define (in the streamline-averaged sense) a range of depths situated below the mixed layer and above topographic influences and where a compensation between mesoscale transient fluxes and the Ekman flux could apply. We provide pictures of the streamline-averaged ACC (Fig20): neither alongstream velocity nor velocity variance show multiple fronts, that are prominent features of sections at any longitude. This happens because streamlines get together in various choke points like Drake passage and therefore continuous, distinct fronts can only be defined in individual basins, not in the circumpolar average. This work continues with the consideration of the density balance and eddy fluxes.

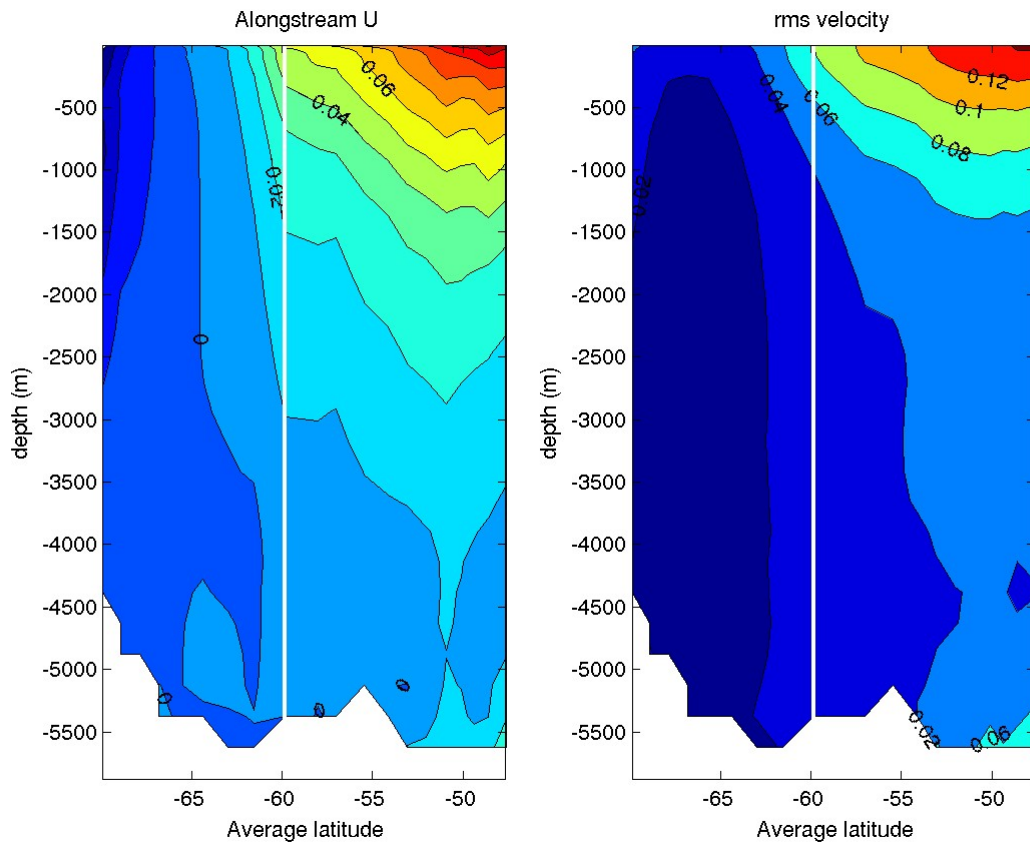


Figure 20: Circumpolar average of alongstream velocity profile (left) and rms velocity (right). The coordinate is the average latitude of each streamline. The white line is the southernmost streamline of the ACC. The picture has been extended southwards to sample all the southern ocean, by linearly interpolating between the southern extension of the ACC and the coastline.

Another collaboration has been developed with Gary Froyland, school of mathematics, at the university of New South Wales. This project, financed by ARC (Australian research council) with the participation of A.M. Treguier and J. Le Sommer, aims at characterizing fronts and mixing with original mathematical methods. A paper using the global $1/4^\circ$ DRAKKAR model has been submitted (Froyland et al, 2006).

References:

- Froyland G., K Padberg, M. H. England, A. M. Treguier, 2006: Detection of coherent oceanic structures via transfer operators, submitted to phys. rev. letter.
- Ivchenko, V.O., K. Richards and D. P. Stevens, 1996: The dynamics of the Antarctic circumpolar current. J. Phys. Oceanogr., 26, 753-774.
- Marshall, J. and T. Radko (2003) Residual mean solutions for the Antarctic Circumpolar Current and its associated overturning circulation. J Phys. Oceanogr. 33 (11): 2341-2354

4.4. Regional model configurations

Many scientific objectives of the DRAKKAR project require regional configurations. The first regional configuration to be set up was NATL4, covering the North Atlantic and Nordic seas (Theetten, 2004). So far this configuration has been implemented with closed boundaries. It has been used for extensive tests that are not detailed in the present report: for example tests of

forcing fields (report by F. Nicolas, 2005) or effects of topography and parameterizations on the overflows (report by R. Almar, 2005). NATL4 has been used for modelling the isotopic composition of Neodymium, in collaboration with scientists at LEGOS and LSCE (section 4.4.1). It has been adapted to support AGRIF zooms (development of the AMEN configuration, section 4.4.2).

Two other regional configurations, with open boundaries, are being used within the DRAKKAR team. The first one is ITF025, a $1/4^\circ$ local model of the Indonesian throughflow (PhD of A. Koch Larrouy, LOCEAN, section 4.4.3) and the second one is a $1/12^\circ$ model of the Gulf of Guinea (PhD of C. Guiavarch, LPO, section 4.4.4).

4.4.1. AMEN configuration (Atlantic Mode water in Embedded model using Nemo/agrif)

This work is aimed at the study of the formation and subduction of subpolar mode water (SPMW), and especially the influence of mesoscale turbulence and direct atmospheric forcing. The properties of subtropical mode waters are correlated with the atmospheric North Atlantic Oscillation (NAO); we want to find out whether similar correlations exist with the properties of SPMW. The numerical model complements studies based on observations of ARGO floats and OVIDE hydrography (Thierry et al, 2006).

The AMEN model configuration is based on NATL4, with a grid refinement between the North Atlantic current and the Azores front, between 0°W and the mid-Atlantic ridge. The grid refinement is based on the new parallel version of the AGRIF code implemented in NEMO (L. Debreu, J.M. Molines). A lot of preliminary work has been necessary in 2005 and early 2006 to validate this new code and to ensure its portability on different machines.

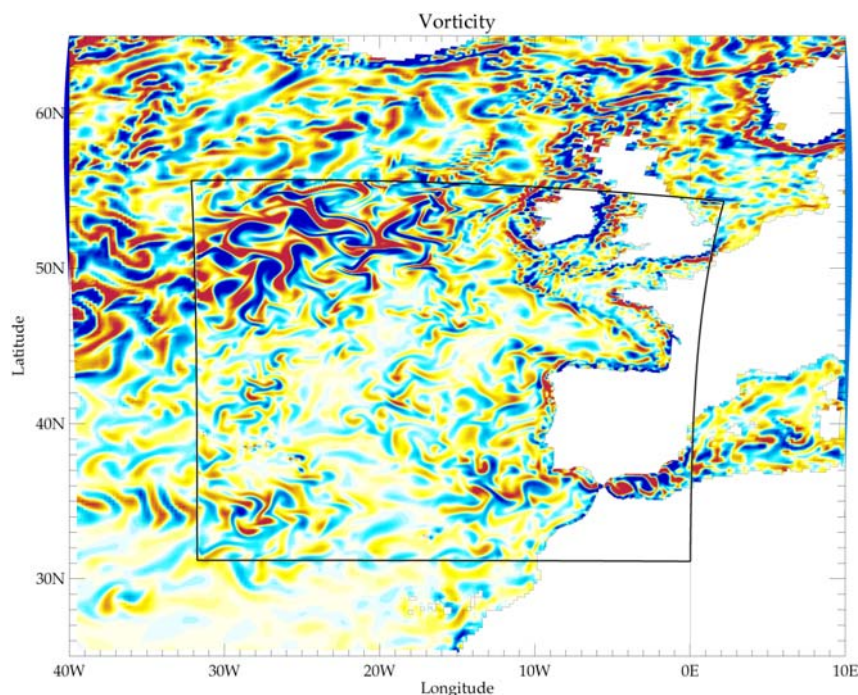


Figure 21: Snapshot of the upper ocean relative vorticity field in the AMEN configuration, featuring the $1/4^\circ$ NATL4 with a grid refinement at $1/12^\circ$ with AGRIF in the intergyre zone (marked by the square box).

For an accurate representation of mode waters and flow-topography interaction we use a refined vertical grid (64 levels instead of 46 in previous DRAKKAR configurations). This grid has been designed in concertation with colleagues at the National Oceanography Centre in Southampton; it is very similar to the grid currently used in the OCCAM model. The bathymetry and the runoff

data are extracted from the NATL12 1/12° configuration of MERCATOR-ocean, which covers the same domain as NATL4. The preparation of bathymetry and initial conditions requires special care to ensure compatibility of the refined region with the rest of the domain. This is performed by a software package called "nesting tools" developed by L. Debreu et al. As the first users of this package we have contributed to its development. The AMEN configuration is running on 64 processors of the IBM zahir at IDRIS; a few years of experiment and a validation will be performed before the end of 2006.

4.4.2. Simulation of the isotopic composition of Neodymium.

Drakkar was not leader in this study, but A.M. Treguier contributed to the simulations. This is an example of cooperation with associated scientists. (S. Peronne, T. Arsouze, A.M. Treguier, C. Jeandel, F. Lacan, JC Dutay).

The oceanic water masses differ by their temperatures, salinity, but also a number of geochemical tracers characterized by their weak concentrations and their ability to quantify oceanic processes (mixing, scavenging rates etc...). Among these tracers, the Nd isotopic composition (hereafter ϵ_{Nd}) is a (quasi) conservative tracer of water mass mixing in the ocean interior, far from any lithogenic inputs. It has been recently established that exchange of Nd at the oceanic margins could be the dominant process controlling both its concentration and isotopic composition distributions in the ocean. This has been confirmed using the low resolution global ORCA2 model (Arsouze et al., 2006). However, the currents flowing on the ocean margins are not correctly represented in ORCA2, especially in the North Atlantic ocean. The North Atlantic is of particular interest since *i*) it is the area of deep water formation and *ii*) these deep waters are characterized by the most negative ϵ_{Nd} values of the world ocean, which are used as "imprint" of the present and past thermohaline circulation. It is therefore essential to understand how these water masses acquire their ϵ_{Nd} signature.

During a 5-month internship at LPO-Brest, Simon Peronne has used the method of Arsouze et al (2006) to calculate the distribution of ϵ_{Nd} in the DRAKKAR model configuration NATL4. This method is based on a very simple model of the modification of ϵ_{Nd} by interaction at the ocean margins, without a complete modelling of the neodymium concentration itself (this would require a full carbon cycle model). First, two 20-years "on-line" experiments have been run. Longer experiments being required to equilibrate the concentration, we have used the dynamical fields of one of these experiments to perform a 150 years "offline" simulation. The new version of TOP (the tracer component of NEMO) has been used, and we have found necessary to modify the input/output strategy to run efficiently on 54 processors of the Zahir machine at IDRIS.

Simulated ϵ_{Nd} distributions have been compared to the present-day data base, vertical profiles, and the results of the low resolution model ORCA2. The eddy permitting model generally provides improved results, when a high enough exchange rate of ϵ_{Nd} is imposed in the deep ocean. Deficiencies of the simulated distribution in the Nordic Seas and the subpolar gyre are explained by errors in the input function on the margins of the Iceland-Scotland Ridge and south of Iceland. The model does not account for all the complexity of the ϵ_{Nd} profiles observed downstream of Denmark Strait and in the Labrador Sea. This is partly due to the representation of the deep western boundary currents, still marginally resolved in this eddy-permitting model.

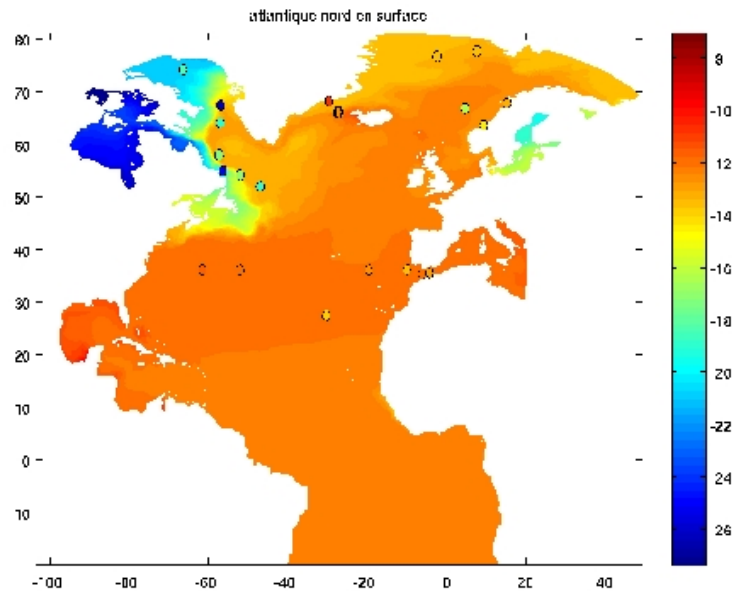


Figure 22: Neodymium isotopic composition ϵ_{Nd} (it is a dimensionless number), after a 150 year offline experiment with the NATLA model. The field is mapped at the surface, and compared with recent observations indicated by circles. The model reproduces low values in the Labrador current, and the ϵ_{Nd} in the subtropical gyre is much more realistic than with the ORCA2 model.

4.4.3. Water mass transformations in the Indonesian throughflow

This study is the topic of the PhD of Ariane Koch-Larrouy, working with Gurvan Madec at LOCEAN, Paris. The first aim was to examine the influence of mixing parameterizations and especially tidal mixing on the properties of the water masses that cross the Indonesian Throughflow. A regional configuration with open boundaries (ITF025) has been set up in order to be able to run a large number of sensitivity studies. The configuration is extracted from the global DRAKKAR configuration and uses the same grid. It is forced at the boundaries by outputs of ORCA025, with slight modifications of the temperature and salinity of some input water masses. Preliminary studies have shown the need for adjustments of the bathymetry (figure...) that have led to considerable improvements of the circulation. The total transport of the throughflow has not changed, but the repartition of the flow across the different passages has become much more realistic.

Even after those improvements, the ITF025 configuration failed to reproduce the intense mixing that is observed in the region. The incoming warm Pacific waters undergo strong transformations that have been attributed to internal tides that are confined within this semi-enclosed area. A specific parameterization has been built to mimic this process. The power converted from barotropic tides into baroclinic tides is constrained by tidal model results while the vertical dependency of energy dissipation is inferred from a 2D internal tide generation model. The model is significantly improved in most of the Indonesian basins, which suggests that the spatial distribution of the eddy diffusivity is adequately prescribed by the new parameterization. These results are described in a paper submitted to Geophysical Research Letters (Koch Larrouy et al, 2006).

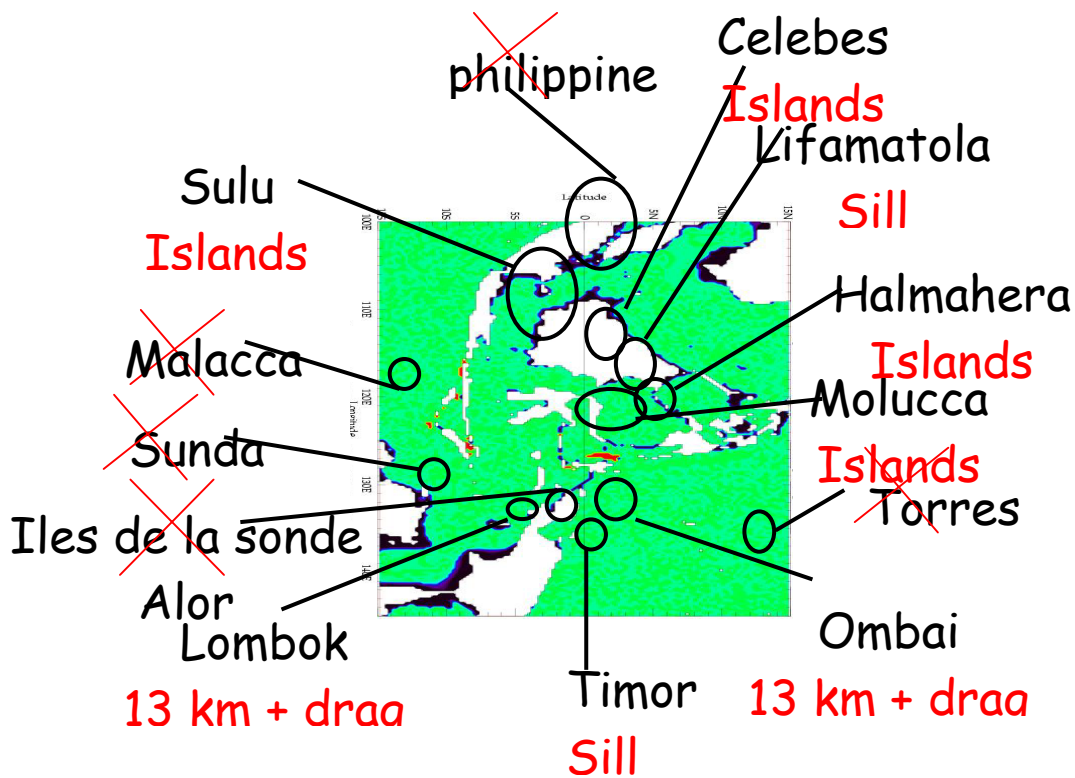


Figure 23: Schematics of the adjustments made to the grid and topography of the global $1/4^\circ$ model in the ITF region. Some passages have been closed (red cross), islands have been restored, sill depths have been adjusted, the grid width and lateral friction drag have been modified in some places.

4.4.4. Modelling biweekly oscillations in the Gulf of Guinea

This study is the topic of the PhD of Catherine Guivarc'h, supervised by A.M. Treguier and A. Vangriesheim at LPO. The aim is to understand the origin of biweekly current oscillations that have been observed on the continental slope off Angola at 1300m depth (Vangriesheim et al, 2005). We have found that a high resolution model ($1/12^\circ$ grid and 70m thick layers near the bottom) greatly improves the representation of the currents trapped to the topography. The GUINEA model configuration is forced at the boundaries by another regional configuration, NATL4; this allows us to use the same forcing for both the large scale and the local model and to generate daily boundary data. The main result of the study is that 95% of the biweekly energy found at the observation site is due to equatorial yanai waves that propagate eastward to the African coast and then south. The Yanai waves are forced by equatorial winds. The map of rms velocity at 1160m (Figure) represents well this phenomenon, and underlines the large assymetry between the amount of energy propagating north and south along the coast. This effect is mainly due to the coastline geometry. Two publications are in preparation.

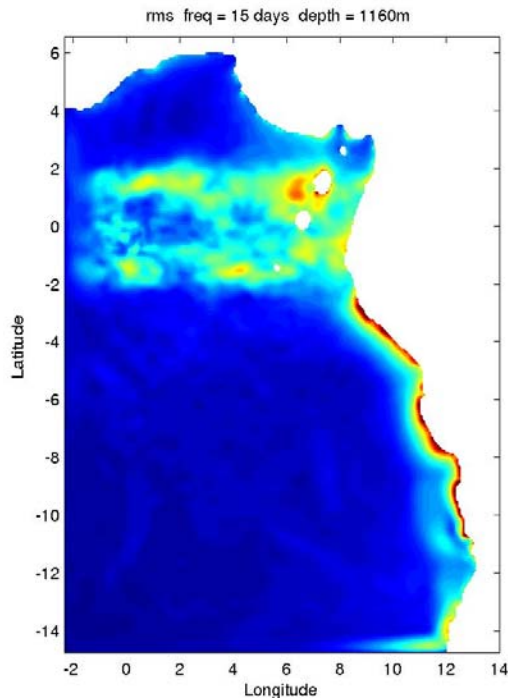


Figure 24: rms velocity for periods close to 15 days in the GUINEA model at 1160m depth. The energy near the equator is due to Yanai waves. The energy concentrates along the coast as the waves propagate south as coastal trapped waves (similar to coastal Kelvin waves).

reference:

Vangriesheim A., A.M. Treguier, and G. Andre, 2005: Biweekly current oscillations on the continental slope of the Gulf of Guinea. *Deep Sea Res.*, 52,11, 2168-2183.

4.5. Studies carried out with Associate Scientists

We present here the abstract of several studies carried out in a close cooperation between Associated Scientists and the DRAKKAR project.

4.5.1. Transient Tracers

Off line calculations of the global ocean distributions of CFC-11, CO₂ and $\Delta^{14}\text{C}$ using ORCA2 and ORCA05 outputs have been performed at LSCE (Lachkar, Orr) to ask what role do eddies play in ocean uptake, storage, and meridional transport of transient tracers. We made global anthropogenic transient tracer simulations in non-eddy (2°cos ϕ ×2°, ORCA2) and eddy (1/2°cos ϕ ×1/2°, ORCA05) versions of the ocean general circulation model OPA9. We focus on the Southern Ocean where tracer air-sea fluxes are largest. Eddies have little effect on global and regional bomb $\Delta^{14}\text{C}$ uptake and storage. Yet for anthropogenic CO₂ and CFC-11, increased eddy activity reduces southern extra-tropical uptake by 28% and 25% respectively. There is a similar decrease in corresponding inventories, which provides better agreement with observations. With higher resolution, eddies strengthen upper ocean vertical stratification and reduce excessive ventilation of intermediate waters by 20% between 60°S and 40°S. By weakening the Residual Circulation, i.e., the sum of Eulerian mean flow and the opposed eddy-induced flow, eddies reduce the supply of tracer-impoverished deep waters to the surface near the Antarctic divergence, thus reducing the air-sea tracer flux. Consequently, inventories for both CFC-11 and anthropogenic CO₂ decrease because their mixed layer concentrations in that region equilibrate with the atmosphere on relatively short time scales (15 days and 6 months, respectively); conversely, the slow air-sea equilibration of bomb $\Delta^{14}\text{C}$ of 6 years, gives surface waters little time to exchange with the atmosphere before they are subducted.

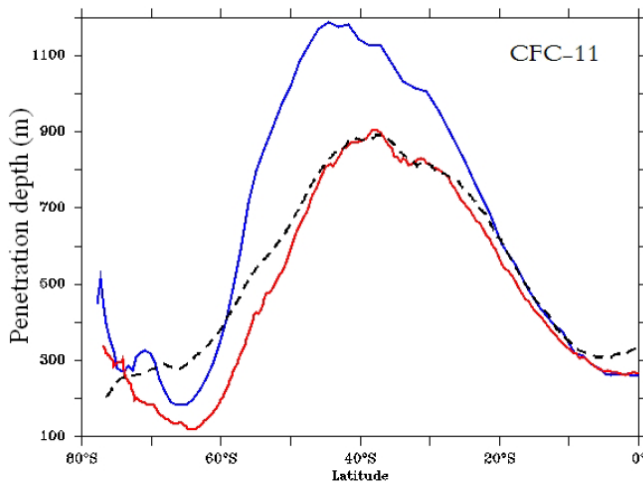


Figure 25: Zonal mean of CFC-11 penetration depth (in m) as observed (black dashes, GLODAP) and as simulated by the eddying (red) and the non-eddying (blue) model over the Southern Hemisphere. The penetration depth of a tracer is defined as the tracer inventory divided by its surface concentration (after Lackhar et al., 2006).

4.5.2. Ensemble study of the vertical transmission of atmospheric induced temperature anomalies

DRAKKAR was not leading this study carried out by M. Lucas and N. Ayoub during their stay at LEGI. Interaction with the DRAKKAR team has been very strong, in Brest and Grenoble, around the NATL4 configuration, and the interpretation of the results. This is an example of a good cooperation with associated scientists.

The penetration of atmospheric forcing into the ocean is a fundamental issue in physical oceanography and climate research. In this study, we use an ensemble method with fifty 7-months (September to March) primitive equation $\frac{1}{4}^\circ$ integrations to investigate the processes that control the vertical transmission of the atmospheric signal into the ocean, focusing principally on its impact on the upper oceanic temperature field. The ensemble is generated by perturbing the wind, atmospheric temperature and incoming solar radiation of the ERA40 reanalysis. Each perturbation consists of a random combination of the first twenty EOFs of the difference between the ERA40 and NCEP/CORE reanalysis data sets. The ensemble standard deviation of various interfacial and oceanic quantities is then examined in the upper 200 metres of 3 distinct regions of the North Atlantic: the Gulf stream, the equatorial band and the North east Atlantic. These show that even a very small perturbation can lead to significant changes in the ocean properties and that regions of oceanic mesoscale activity are the most sensitive. The transmission is driven by the vertical diffusivity and the eddy activity. The role of subsurface currents is also crucial in carrying the eddy signal away from the regions of mesoscale activity. Finally, the decorrelation time scale of the mesoscale activity is critical in determining the amplitude of the oceanic response.

4.5.3. Agrifmex

To develop and validate the MPI version of the new AGRIF grid refinement package, an application has been made (PhD of J. Jouano) in cooperation with CICESE at Ensenada in Mexico (J. Sheinbaum, J. Candela). The NATL3 configuration inherited from CLIPPER (similar to NATL4 but extending only to 70°N and with a resolution of $\frac{1}{3}^\circ$) is used. The configuration has been updated to NEMO. A grid refinement to $\frac{1}{15}^\circ$ using the new MPI version of AGRIF is applied to the Caribbean Sea and the Gulf of Mexico (CARIB15, Fig. 26). This configuration is referred to as AGRIFMEX.

The objective is to identify the main source of the Caribbean Eddies: are they the continuity of the North Brazil Current eddies after they pass through the lesser Antilles, or are they locally generated by Baroclinic instability. This study requires both a high resolution in the Caribbean Sea to resolve instability processes, and a correct representation of the remote forcing by the tropical Atlantic ocean. The grid refinement approach in an Atlantic model configuration thus appear quite well suited. The AGRIFMEX configuration was first implemented at the IDRIS computer centre, then on the PC cluster of CICESE. Results from model simulation show that the relevant dynamical processes are well simulated by the model (Fig. 26), and suggest that the local baroclinic instability is a major driver of the Caribbean Eddies (Fig. 27).

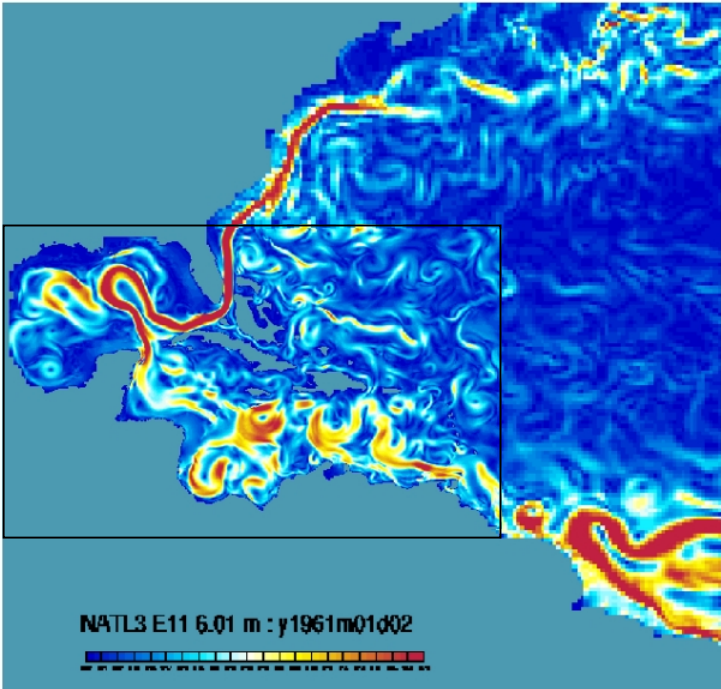


Figure 26. Snapshot of current velocity in the AGRIFEX configuration (yellow colour indicate velocities of 40 cm/s, and red colour velocity of 70 cm/s or higher). The area refined to 1/15° is the black rectangle. Outside, the resolution is 1/3°, a resolution which allows the generation of NBC eddies. Large eddies can be seen in the Caribbean Sea.

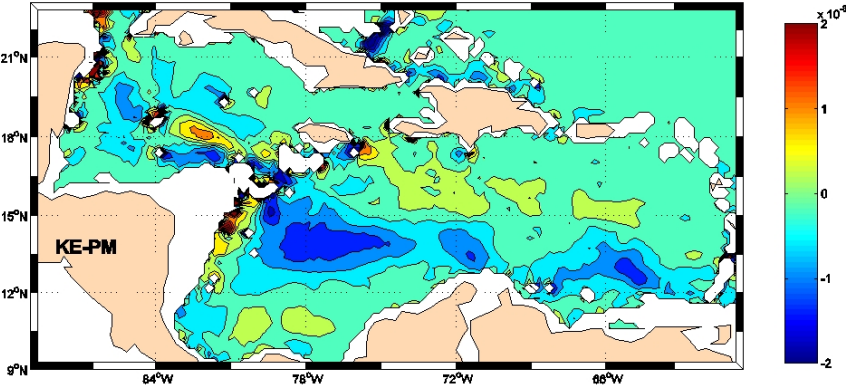


Fig. 27: Rate of baroclinic energy conversion (i.e. transfer between mean potential energy (mpe) and eddy kinetic energy (eke) between 80 m and 280 m). Negative values indicate that baroclinic instability extract eddy energy from the mean stratification. This term being dominant in the energy balance, suggests that the local instability plays a major role in the growth of the Caribbean Eddies.

5. DRAKKAR Publications in 2006

Peer Review Journals

- Barnier B., G. Madec, T. Penduff, J.-M. Molines, A.-M. Treguier, J. Le Sommer, A. Beckmann, A. Biastoch, C. Böning, J. Dengg, C. Derval, E. Durand, S. Gulev, E. Remy, C. Talandier, S. Theetten, M. Maltrud, J. McClean, and B. De Cuevas, 2006: Impact of partial steps and momentum advection schemes in a global ocean circulation model at eddy permitting resolution. *Ocean Dynamics*, Vol 4, DOI 10.1007/s10236-006-0082-1.
- Béranger K., B. Barnier, S. Gulev and M. Crépon, 2006 : Comparing twenty years of precipitation estimates from different sources over the world ocean. *Ocean Dynamics*, Vol. 56-2, 104-138, DOI: 10.1007/s10236-006-0065-2 2006.
- Gulev S.K., Barnier B., Molines J.-M., and Penduff T., 2006: Impact of spatial resolution on simulated surface water mass transformation in the Atlantic. *Ocean Modelling*, submitted.
- Koch-Larrouy A., G. Madec, P. Bouruet-Aubertot, T. Gerkema, L. Bessières, and R. Molcard, 2006: On the transformation of Pacific Water into Indonesian ThroughFlow Water by internal tidal mixing, submitted to *Geophysical Research Letters*.
- Lachkar Z., J. C. Orr, J.-C. Dutay, and P. Delecluse, 2006: Effects of mesoscale eddies on global ocean distributions of CFC-11, CO₂ and $\Delta 14\text{C}$. *Ocean Sciences*, in révision.
- Le Sommer J, Penduff T, Madec G (2006) How momentum advection schemes affect current-topography interactions in the DRAKKAR 1/4-degree z-coordinate model. Submitted to *Ocean Modelling*;
- Lucas M., N. Ayoub, B. Barnier, T. Penduff, and P. de Mey, 2006: Vertical transmission of the atmospheric induced temperature anomaly: an ensemble study. To be submitted to *Ocean Modelling*.
- Penduff T., J. Le Sommer, B. Barnier, A.-M. Treguier, J.-M. Molines, and G. Madec, 2006: Depth-dependant effects of momentum advection, sidewall boundary conditions, and partial steps topography in 1/4° global ocean simulations, To be submitted to *Ocean Modelling*.

Newsletters and Proceedings

- Ayoub N., M. Lucas, B. Barnier, T. Penduff, G. Valladeau, and P. De Mey, 2006: A study of model errors in surface layers due to uncertainties in the atmospheric forcing fields, *Lettre trimestrielle Mercator* No 22, Juillet 2006, p 29-38.
- Barnier B., Brodeau L., et Penduff T.: Ocean Surface Forcing and Surface Fields. *Lettre trimestrielle Mercator* No 22, Juillet 2006, p 4-7.
- Molines J.M., A.M. Treguier, B. Barnier, L. Brodeau, J. Le Sommer, G. Madec, T. Penduff, S. Theetten, Y. Drillet, C. Talandier, J. Orr, Z. Lachkar Le modèle DRAKKAR de la variabilité océanique globale, 1958-2004. à paraître dans la Lettre de l'IDRIS, Novembre 2006.
- Penduff T., 2006: DRAKKAR : modélisation à haute résolution de la variabilité océanique au cours des 50 dernières années. DRAKKAR : high-resolution modeling of ocean variability over the last 50 years, *Lettre PIGB-PMRC, No19*, Mai 2006, p 15-21.
- Brodeau L., T. Penduff, and B. Barnier, 2006: Sensitivity of DRAKKAR global simulations to two existing and a hybrid atmospheric forcing functions. *Proceedings of the Radar Satellite Altimetry Colloquium*, March 13-17, Venice, Italy;
- Penduff T., B. Barnier, A.-M. Treguier, and P.-Y. Le Traon, 2006: Synergy between ocean observations and numerical simulations: CLIPPER heritage and DRAKKAR perspectives, *Proceedings of the Radar Satellite Altimetry Colloquium*, March 13-17, Venice, Italy

Communications at international colloquiums

- Barnier B., 2006: Impact of partial steps and momentum advection schemes in a global ocean circulation model at eddy permitting resolution, *MERSEA Annual Science Meeting*, March 6-7, London.
- Barnier B., 2006: Recent progresses in modelling the ocean general circulation at eddy permitting resolution, *Radar Satellite Altimetry Colloquium*, March 13-17, Venice, Italy.
- Brodeau L., T. Penduff, B. Barnier, A.M. Treguier, S. Gulev, and J.M. Molines, 2006: Combining satellite products and reanalysed atmospheric variables to build long-term forcing for global ocean/sea-ice simulations, *Geophysical Research Abstracts, Vol. 8*, 07880, 2006 EGU General Assembly 2006, Vienna, 2-7 avril.
- Lachkar Z., J.C. Orr, J.C. Dutay and P. Delecluse, 2006: Effect of ocean mesoscale eddies on global

- distributions of CFC-11, C-14, and CO₂, *Geophysical Research Abstracts*, Vol. 8, 06717, 2006, EGU General Assembly 2006, Vienna, 2-7 avril.
- Le Sommer J., T. Penduff, G. Madec, S. Theetten and B. Barnier, 2006: What does vertical velocity tell about the behavior of numerical schemes? *Geophysical Research Abstracts*, Vol. 8, 09532, 2006, EGU General Assembly 2006, Vienna, 2-7 avril.
- Mathiot P., B. Barnier, H. Gallée, J.M. Molines and T. Penduff, 2006: On the role of katabatic winds in the formation of Antarctic Bottom Waters, *Geophysical Research Abstracts*, Vol. 8, 07356, 2006, EGU General Assembly 2006, Vienna, 2-7 avril.
- Peronne S., A.M. Treguier, T. Arsouze, JC Dutay, F. Lacan, C. Jeandel, 2006: Modelling the oceanic Nd isotopic composition with a North Atlantic eddy permitting model. Abstract, AGU meeting, november 2006.
- Penduff T., L. Brodeau, M. Juza, and B. Barnier, 2006: Hybridizing satellite products and reanalyzed atmospheric fields for the forcing of long-term ocean/sea-ice DRAKKAR simulations, OST/ST meeting March 17, Venice, Italy.

Project reports

- Peronne S., 2006: Simulation numérique du Néodyme dans l'Atlantique Nord. Rapport de stage de fin d'étude, ISITV, Université du Sud Toulon Var, La Garde Cedex, 110 pp.
- Bourdallé-Badie R., and A. M. Treguier, 2006: A climatology of Runoff for the global ocean-ice model ORCA025. Mercator Ocean Reference: MOO-RP-425-365-MER, 28 pp.
- Molines J. M., B. Barnier, T. Penduff, L. Brodeau, A.M. Treguier, S. Theetten, and G. Madec, 2006: Definition of global $\frac{1}{2}^\circ$ experiment with CORE interannual forcing, ORCA05-G50. *LEGI internal report*, 27 pp.
- Molines J. M., B. Barnier, T. Penduff, L. Brodeau, A.M. Treguier, S. Theetten, and G. Madec, 2006: Definition of a 45 years interannual experiment ORCA025-G70. *LEGI internal report*, 34 pp.
- Treguier A.M., J.M. Molines, G. Madec, 2006: Meridional circulation and transports in ORCA025 climatological experiments. *Report LPO-06-02*, 23 pp.

6. Personnel

Ayoub Nadia	CR CNRS	LEGI/LEGOS	30%
Barnier Bernard	DR CNRS	LEGI	90%
Madec Gurvan	DR CNRS	LODYC	15%
Orr James	DR CNRS	LSCE	30%
Penduff Thierry	CR CNRS	LEGI	90%
Thierry Virginie	Chercheur IFREMER	LPO	50%
Treguier Anne Marie	DR CNRS	LPO	90%
Wirth Achim	CR CNRS	LEGI	20%
<i>Collaborateurs techniques</i>			
Brasseur Josiane	Secrétariat	LEGI	40%
Molines Jean Marc	IR1 CNRS	LEGI	80%
Theetten Sébastien	IE CNRS	LPO	90%
<i>Postdoctorants et ingénieurs contractuels</i>			
Le Sommer Julien	PostDoc UE	LEGI	100%
Juza Mélanie	Ingénieur CNES/INSU	LEGI	100%
Marc Lucas	PostDoc SHOM	LPO	100%
<i>Etudiants en thèse</i>			
Brodeau Laurent	Thèse	LEGI	100%
Guiavarc'h Catherine	Thèse	LPO	30%
Hervieux Gaëlle	Thèse	LEGI	100%
Koch-Larrouy Ariane	Thèse	LOCEAN	100%
Lackhar Zouhair	Thèse	LSCE	50%
Mathiot Pierre	Thèse	LEGI/LGGE	100%
<i>Etudiants stagiaires</i>			
Lecointre Albanne	DEA	LEGI	100%

Acknowledgements

Support to DRAKKAR comes from various grants and programs listed hereafter. French national programs GMMC, LEFE, and PICS 2475 from Institut National des Sciences de l'Univers (INSU) and Centre National de la Recherche Scientifique(CNRS). European integrated project MERSEA. Support from CNES and marché EPSHOM-UBO 02.87.024.00.470.29.25 are acknowledged. Computations presented in this study were performed at Institut du Développement et des Ressources en Informatique Scientifique (IDRIS).

Liste of Annexes

ANNEX 1 : Le modèle DRAKKAR de la variabilité océanique globale, 1958-2004. To appear in IFRIS Newsletter.

ANNEX 2: Synergy between ocean observations and numerical simulations: Clipper heritage and Drakkar perspectives. Proceeding of Symposium on 15 years of Progress in Radar Altimetry. Venice, 13-18, March 2006.

ANNEX 3 : DRAKKAR, modélisation à haute résolution de la variabilité océanique au cours des 50 dernières années. Lettre du PIGB N°19, May 2006.

ANNEX 4 : Impact of partial steps and momentum advection schemes in a global ocean circulation model at eddy permitting resolution. Ocean Dynamics, November 2006.

ANNEX 5: Ocean surface forcing and surface fields. Mercator News Letter, July 2006.

ANNEX 6: A study of model errors in surface layers due to uncertainties in the atmospheric forcing fields Mercator News Letter, July 2006.

ANNEX 7: Sensitivity of DRAKKAR global simulations to two existing and a hybrid atmospheric forcing functions. Proceeding of Symposium on 15 years of Progress in Radar Altimetry Venice, 13-18 Mars 2006.

ANNEX 8: Comparing 20 years of precipitation estimates from different sources over the world ocean. Ocean Dynamics, April 2006.

TECHNICAL ANNEX 1: A Climatology of Runoff for the global ocean-ice model ORCA025. Mercator-Ocean Technical note, August 2006.

TECHNICAL ANNEX 2: Definition of the global 1/2° experiment with CORE interannual forcing ORCA05-G50. LEGI Technical note, November 2006.

TECHNICAL ANNEX 3: Definition of the interannual experiment ORCA025-G70 1958-2004. LEGI Technical note, November 2006.